January 2017

Hubble Space Telescope Primer for Cycle 25

An Introduction to the HST for Phase I Proposers

STScI | SPACE TELESCOPE SCIENCE INSTITUTE

3700 San Martin Drive
Baltimore, Maryland 21218
help@stsci.edu

Operated by the Association of Universities for Research in Astronomy, Inc., for the National Aeronautics and Space Administration

How to Get Started

For information about submitting a HST observing proposal, please begin at the Cycle 25 Announcement webpage at:

http://www.stsci.edu/hst/proposing/docs/cycle25announce

Procedures for submitting a Phase I proposal are available at:

http://apst.stsci.edu/apt/external/help/roadmap1.html

Technical documentation about the instruments are available in their respective handbooks, available at:

http://www.stsci.edu/hst/HST_overview/documents

Where to Get Help

Contact the STScI Help Desk by sending a message to help@stsci.edu. Voice mail may be left by calling 1-800-544-8125 (within the US only) or 410-338-1082.

The *HST Primer for Cycle 25* was edited by Susan Rose, Senior Technical Editor and contributions from many others at STScI, in particular John Debes, Ronald Downes, Linda Dressel, Andrew Fox, Norman Grogin, Katie Kaleida, Matt Lallo, Cristina Oliveira, Charles Proffitt, Tony Roman, Paule Sonnentrucker, Denise Taylor and Leonardo Ubeda.

Send comments or corrections to:
Hubble Space Telescope Division
Space Telescope Science Institute
3700 San Martin Drive
Baltimore, Maryland 21218
E-mail:help@stsci.edu

CHAPTER 1:

Introduction

In this chapter...

1.1 About this Document

The *Hubble Space Telescope Primer for Cycle 25* is a companion document to the *HST Call for Proposals*[1]. It provides an overview of the Hubble Space Telescope (HST), with basic information about telescope operations, instrument capabilities, and technical aspects of the proposal preparation process. A thorough understanding of the material in this document is essential for the preparation of a competitive proposal.

This document is available as an online HTML document and a PDF file. The HTML version, optimized for online browsing, contains many links to additional information. The PDF version is optimized for printing, but online PDF readers have search capabilities for quick retrieval of specific information.

1.2 What's New This Cycle

The following instruments will be offered in Cycle 25: two cameras on ACS (ACS/WFC and ACS/SBC), COS, FGS, STIS, and WFC3.

1. The *HST Call for Proposals* discusses the policies and procedures for submitting a Phase I proposal for *HST* observing or archival research.

Due to heavy demand and the need for scheduling flexibility in Cycle 25, Large GO programs requesting 75 orbits or more must use the shorter orbital visibility values from Table 6.1; this will be enforced for such programs approved for Phase II.

COS/FUV

COS Lifetime Position. In the Summer of 2017, the COS FUV spectra will be moved from lifetime position 3 (LP3) to lifetime position 4 (LP4) in order to alleviate the continuing effects of gain sag. Typical spectral resolution ($\lambda/\Delta\lambda$) is expected to decline by about 15% for observations with the primary science aperture (PSA). Changes in the COS extraction and calibration pipeline have improved the calibration of point-source observations. COS/FUV observations at LP3 and LP4 targeting extended objects or using the Bright Object Aperture (BOA) are more complex. In these cases the standard pipeline calibration will not always produce the flux accuracy achieved for point sources observed with the PSA, and it will be the responsibility of the user to evaluate the adequacy of the spectral extraction and, if necessary, undertake any customized extractions. See Chapter 3 of the *COS Data Handbook* for more information.

STIS/CCD

For Cycle 25 STIS/CCD imaging observations. Observations with the BAR5 coronagraphic position in concert with specific observing strategies can obtain contrasts for faint point sources of 10^{-6} beyond 0.55". For more information, see Section 4.6.4, and Section 12.11 of the *STIS Instrument Handbook*.

For Cycle 25 STIS spectroscopy with aperture widths smaller than 0.2". There is some evidence that in recent years the STIS instrument focus has changed. Because the STIS corrector mechanism has not been moved since 1997, it is unlikely that the focus will be adjusted unless the performance suffers from additional degradation.

1.3 Resources, Documentation and Tools

1.3.1 Phase I "Roadmap"

The Phase I Proposal Roadmap is a high level step-by-step guide to writing a Phase I Proposal. At each step, links are provided to relevant information.

1.3.2 Cycle 25 Announcement Webpage

They Cycle 25 Announcement webpage contains links to information needed for preparing a *HST* proposal. It also contains late-breaking updates regarding the Phase I process and a FAQ (frequently asked questions).

1.3.3 Cycle 25 *Call for Proposals*

The *Call for Proposals* discusses policies and procedures for submitting a Phase I proposal for *HST* observing or Archival Research. It also provides a summary of the proposal process from proposal submission to the execution of observations. The *Call for Proposals* document is available at the Cycle 25 Announcement webpage.

1.3.4 Instrument Handbooks

Instrument handbooks, the primary source of information for *HST* instruments, provide additional information beyond what's presented in this *Primer*. Please use current versions of the handbooks when preparing the Phase I proposal. The latest handbook versions for active and decommissioned instruments are available at the HST Documents webpage. Other potentially useful documents, such as instrument science reports, data handbooks, and calibration conference proceedings are also accessible from that website.

1.3.5 The Astronomer's Proposal Tool (APT) and the Aladin Sky Atlas

The Astronomers Proposal Tool (APT) is the software interface for all Phase I and Phase II proposal submissions for *HST*. Please refer to the APT webpage for information regarding the installation and use of APT.

The *Aladin Sky Atlas*, available through APT, can be used to display *HST* apertures on images of the sky. This software interface provides access to a wide variety of images and catalogs; note that the GALEX catalog is available to assist in checking for potentially dangerous objects for the UV detectors. Training documentation and videos can be found on the APT Training Materials webpage.

1.3.6 Exposure Time Calculators (ETCs)

Information in this *Primer*, together with the instrument handbooks, provides the means for estimating acquisition times, exposure times, and other observational parameters. Values provided in document tables, or as illustrations, are only approximations; reliable calculations that take into account the complex telescope and instrument operation are best obtained using software tools provided by STScI, such as the Exposure Time Calculators (ETCs) and APT (Section 1.3.5). The ETCs, for example, provide warnings for target count rates that exceed saturation and safety

limits. Note, however, that Signal-to-Noise (S/N) predictions from the ETCs do not include the effects of degrading CTE (Charge Transfer Efficiency) for CCD detectors.

Descriptions of the ETCs for active instruments, including determinations of exposure time as a function of instrument sensitivity and S/N ratio, are available in these documents: Chapter 9 of the *ACS Instrument Handbook*, Chapter 7 of the *COS Instrument Handbook*, Chapter 6 of the *STIS Instrument Handbook*, and Chapter 9 of the *WFC3 Instrument Handbook*.

1.3.7 *HST* Data Archive

The HST Data Archive is part of the Mikulski Archive for Space Telescopes (MAST). The HST Data Archive contains all the data taken by HST. Completed HST observations from both General Observer (GO) and Guaranteed Time Observer (GTO) programs are available to the community upon the expiration of their proprietary periods. Observations taken by Large, Calibration, Treasury (see Section 3.2.5 of the Call for Proposals and subsections therein), and Large GO Pure Parallel programs (see Section 4.2.2 of the Call for Proposals) generally carry no proprietary period.

The HST Archive webpage provides links to information about getting started, search and retrieval, documentation, etc. (see also the introductory description in Section 7.2). You can search for HST data using either of two main search pages: the dedicated HST search page or the Data Discovery Portal. The Canadian Astronomy Data Centre (CADC) and the European Space Agency Centre (ESAC) maintain copies of the HST science data, and are the preferred sources for Canadian and European astronomers.

The Hubble Legacy Archive (HLA) is a project designed to enhance science from HST data by augmenting the HST Data Archive and by providing advanced browsing capabilities. Features of the HLA include a preview viewer, an interactive image display, a footprint service, individual, combined and mosaicked images, improved astrometric positions, object catalogs, and selected grism extractions. The HLA is a joint project of the Space Telescope Science Institute, the Canadian Astronomy Data Centre (CADC), and the European Space Astronomy Centre (ESAC). Section 7.3 contains more detailed information about the HLA.

The HLA provides source lists for tens of thousands of HST images. The Hubble Source Catalog (HSC) combines these visit-based WFC3, ACS, and WFPC2 source lists from the HLA into a master catalog with roughly 300 million sources. Searches that would have required months or years to perform in the past can be completed in a matter of seconds using the HSC. Version 1 of the HSC was released in February 2015, and Version 2 was released in the Fall 2016. More information about the HSC

can be found in Section 7.4 The HSC is an invaluable resource for exploring a wide range of new archival proposals, a few potential examples of which are included in Section 7.4.

Cycle 25 proposers will be able to mine the HST Spectroscopic Legacy Archive for high-level data products intended to accelerate the scientific use of existing spectroscopic data. This archive will contain "science grade" co-added spectra of all usable public data, combining exposures for each target from across visits, programs, and cycles. This data will be organized into "smart archives" by target type (such as "hot stars" and "white dwarfs") and by scientific purpose ("IGM absorption sources") so that samples can be readily constructed and downloaded without manual interaction with MAST. The first generation of these products for the FUV modes of COS is available online via MAST. We encourage the development and submission of Archival Programs based on these new products.

Questions about the Archive and archival data should be sent to the Archive Help Desk at archive@stsci.edu or 410-338-4547.

1.3.8 Duplication Checking

The HST Data Archive provides access to several tools that allow you to check whether planned observations duplicate any previously executed or accepted HST observations. For details see Section 5.2.2 of the Call for Proposals.

1.3.9 Data Reduction and Calibration

Introduction to the HST Data Handbooks is a general overview of HST data formats and software tools. It complements the instrument data handbooks that contain more details about calibration and data analysis. The latest versions of the instrument data handbooks are available at the Documents webpage.

The Space Telescope Science Data Analysis Software (STSDAS) webpage has links to the software used to calibrate and analyze *HST* data, along with documentation on its use. More details are available in Section 7.1. The *DrizzlePac Handbook* provides information about the DrizzlePac software package that has replaced MultiDrizzle in pipeline calibration and post-pipeline processing. Some information about dither patterns, drizzling, and various observing considerations are included in it, but for more detailed information, please refer to the Phase II Proposal Instructions and instrument handbooks.

1.4 STScI Help Desk

If this *HST Primer* and the materials referenced in it do not answer your questions, or if you have trouble accessing or printing Web documents, please contact the Help Desk. You may do this in either of two ways:

- Send e-mail to help@stsci.edu
- Call 1-800-544-8125 or,
- [1] 410-338-1082 from outside the United States and Canada,

CHAPTER 2:

System Overview

In this chapter...

2.1 Telescope Design and Field of View

The design and layout of *HST* are shown schematically in Figure 2.1. The telescope is powered by two solar arrays that are oriented towards the sun. Nickel-hydrogen batteries power the telescope during orbital night. Two high-gain antennae provide communications with the ground via the Tracking and Data Relay Satellite System (TDRSS). Power, control, and communication functions are carried out by the Support Systems Module (SSM) that encircles the primary mirror.

Scientific instruments (SIs) are mounted in bays behind the primary mirror. WFC3 occupies one of the four radial bays; it has a 45° pick-off mirror that allows it to receive the on-axis beam as shown in Figure 2.2. There are three Fine Guidance Sensors (FGSs), each in the other radial bays, that receive light that is 10 to 14 arcseconds off-axis in the telescope's field of view. At least two FGSs are required to guide the telescope, therefore, it's possible to conduct astrometric observations with the third FGS. The remaining SIs are mounted in the axial bays and receive images several arcminutes off-axis.

The coordinate system used for *HST*'s focal plane is fixed to the telescope; it consists of three orthogonal axes: U1, U2 and U3. As shown in Figure 2.1, U1 lies along the optical axis, U2 is parallel to the solar array rotation axis, and U3 is perpendicular to the solar array axis. (Note: Some *HST* documentation uses the alternative V1, V2, V3 coordinate system for which V1=U1, V2= –U2 and V3= –U3.)

Figure 2.1: The Hubble Space Telescope Configuration after Servicing Mission 4 in 2009

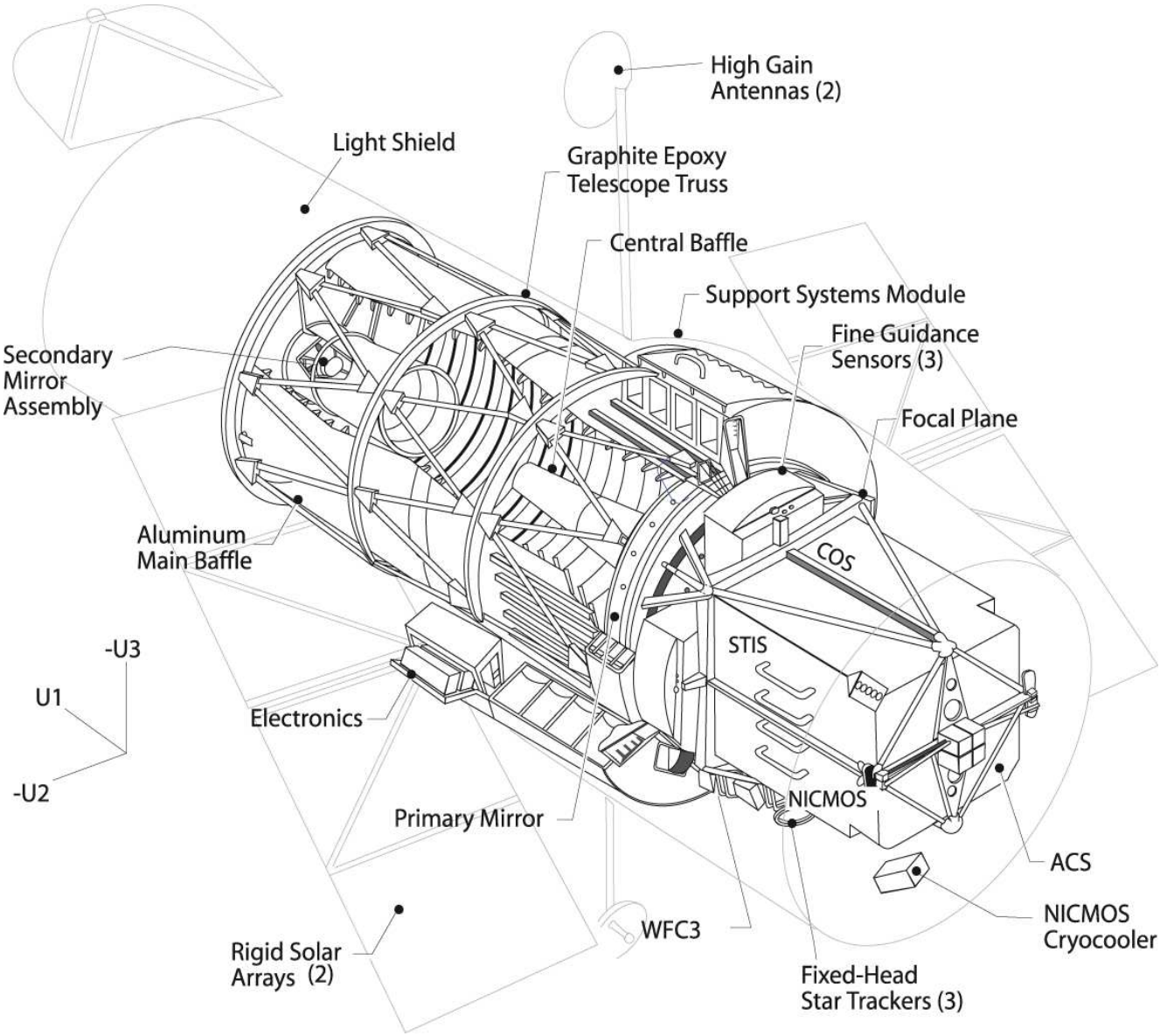

Major components are labeled, and a diagram in the lower left shows the U1,U2, and U3 spacecraft axes.

Figure 2.2: HST Field of View

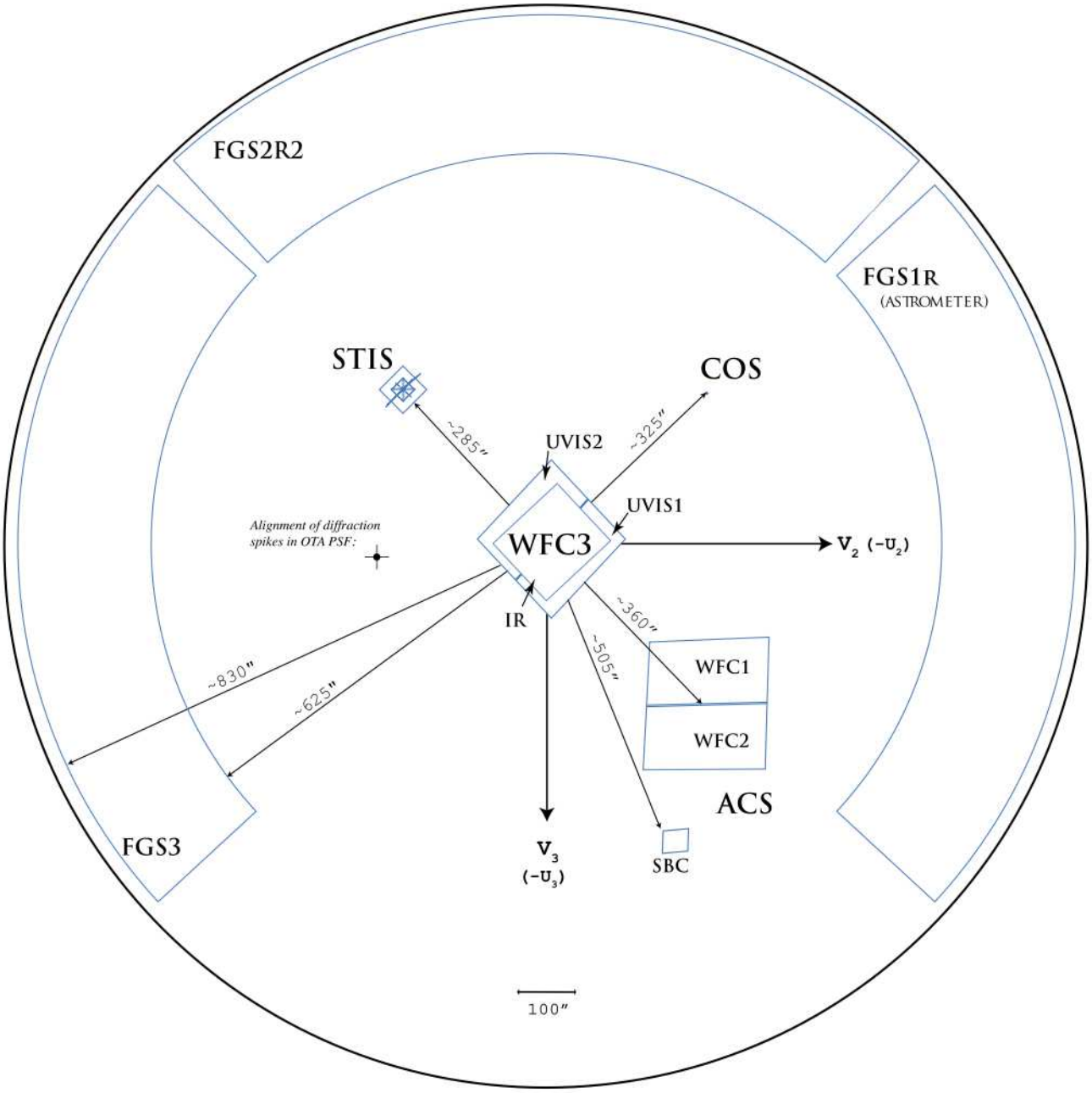

Aperture locations for science instruments and FGSs are shown in the (U2,U3) focal plane, as it would appear projected onto the sky. The scale is in arcseconds.

Table 2.1 lists the rough effective locations of the SI apertures in the (U2,U3) coordinate system. Precise values, available in the HST Instrument Handbooks (see Section 1.3), depend on subtleties in aperture definitions and operational modes.

Table 2.1: Nominal Effective Relative Aperture Locations

Instrument	Aperture	U2 (arcsec)	U3 (arcsec)
ACS	WFC	–259	–239
	SBC	–205	–467
COS		+229	-229
FGS	FGS1R	–722	8
STIS		214	225
WFC3	UVIS	-9	-3
	IR	0	-9

2.2 Orbital Constraints

HST is in a relatively low orbit (less than 600 km above Earth), which imposes a number of constraints upon its observations. As seen from *HST*, most targets are occulted by the Earth for varying lengths of time during each 96-minute orbit. Targets lying in the orbital plane are occulted for the longest interval, about 44 minutes per orbit. These orbital occultations, analogous to the diurnal cycle for ground-based observing, impose the most serious constraint on *HST* observations. (In practice, the amount of available exposure time in an orbit is further limited by Earth limb avoidance limits, the time required for guide star acquisitions or reacquisitions, and instrument overheads.)

2.2.1 Continuous Viewing Zone (CVZ)

The duration of target occultation decreases with a target's increasing angle from the spacecraft's orbital plane. Targets lying within 24° of the orbital poles are not *geometrically* occulted at any time during the HST orbit. This gives rise to so-called Continuous Viewing Zones (CVZs). But note that the actual size of these zones is less than 24° due to the fact that HST cannot observe close to the Earth limb (see Section 2.3).

Since the orbital inclination is 28.5°, any target located in two declination bands near ±61.5° may be in the CVZ at some time during the 56-day *HST* orbital precession cycle. Some regions in these declination bands are unusable during the part of the year when the sun is too close to those regions. The number and duration of CVZ passages depend on the telescope orbit and target position, and may differ significantly from previous cycles. Please refer to the HST Orbital Viewing and Schedulability webpage for information on determining the number and duration of CVZ opportunities in Cycle 25 for a given target location. Also note that the South Atlantic Anomaly (SAA; see Section 2.2.2) limits any *uninterrupted* observation to no more than five to six orbits per day.

The brightness of scattered earthshine background during CVZ observations is not greater than during non-CVZ observations since the same bright earth limb avoidance angle is used. However, the duration of relatively high background can be much longer for CVZ observations than for non-CVZ observations, because the line of sight may continuously graze the bright earth limb avoidance zone during CVZ observations.

In general, CVZ observations should not be requested under normal conditions if observations are limited by sky background. The increased earthshine means that CVZ observations offer virtually no efficiency gain for background-limited broad-band imaging in the optical or infrared. There have been cases in the past (e.g., Hubble Deep Field observations) where optical imaging has been interleaved with other kinds of observations. However, such observations are difficult to schedule and require strong scientific justification. Observers contemplating using CVZ observations are encouraged to contact the STScI Help Desk (see Section 1.3.9). CVZ observations are also generally incompatible with special timing requirements (e.g., timing links, special spacecraft orientations, or targets of opportunity; see Section 4.1.1 of the Call for Proposals for more details).

2.2.2 South Atlantic Anomaly (SAA)

The South Atlantic Anomaly, a lower extension of the Van Allen radiation belts, lies above South America and the South Atlantic Ocean. No astronomical or calibration observations are possible (except for some specialized and infrequently executed WFC3 observations) during spacecraft passage through the SAA because of high background induced in the scientific instruments and FGSs.

As the *HST* orbit precesses and the Earth rotates, the southern part of the *HST* orbit intersects the SAA each day for seven to nine orbits in a row (so-called "SAA-impacted" orbits). These SAA-impacted orbits are followed by five to six orbits (eight to ten hours) without SAA intersections. During SAA orbit intersections, *HST* observing activities must be halted for approximately 20 to 25 minutes, except for the previously mentioned WFC3 observations. This cycle of SAA-impacted orbits and SAA-free orbits lasts approximately 24 hours, so is repeated every day. It affects all observations, including CVZ observations.

Typically, uninterrupted observations can execute in five or six orbits before they have to be halted due to *HST* passage through the SAA. STIS MAMAs and the ACS/SBC have tighter operating constraints than other instruments in that they cannot be operated in an orbit that is even partially impacted by the SAA. *These detectors can only be used during the five to six orbits each day that are completely free of SAA intersections.* (This restriction does not apply to COS.) Some WFC3 science observations are allowed during SAA passage (e.g., planetary occultations and transits). Please refer to WFC3 ISR 2009-40 and WFC3 ISR 2009-47 for more information about detailed studies of WFC3 camera operations during SAA passage.

2.2.3 Predicted HST Position

Atmospheric drag on the spacecraft is a significant issue because *HST* is in a low Earth orbit. Moreover, the amount of drag varies depending on the orientation of the telescope and the density of the atmosphere (which, in turn, depends on the level of solar activity). Consequently, it is difficult to predict in advance where *HST* will be in its orbit at a given time. For instance, the predicted position of the telescope made two days in advance can be off by as much as 30 km from its actual position. An estimated position 44 days in the future may be off by ~4000 km (95% confidence level).

Positional uncertainty can affect observations of time-critical phenomena and near-Earth solar system bodies. In the former case, a target could be behind Earth during the event so it may not be known if a given event will be observable until a few days before the observation. In the latter case, positional uncertainty could introduce uncertainties in the parallax correction.

2.3 Pointing Constraints

HST uses electrically driven reaction wheels to perform all slewing required for guide star acquisition and pointing control. A separate set of rate gyroscopes provides attitude information to the pointing control system (PCS). The slew rate of *HST* is limited to approximately 6° per minute of time. Consequently, about one hour is needed to go full circle in pitch, yaw, or roll. After the telescope arrives at the new target, attitude updates and guide star acquisitions take an additional 13 minutes**.** As a result, large maneuvers are costly in time and are generally scheduled during Earth occultation or while crossing the SAA (see Section 2.2.2).

The target-to-sun angle at the time of observation must be greater that 50°. Exceptions, however, have been made to these rules under three-gyro operations. For example, observations of Venus and a comet were cautiously obtained with the sun angle being slightly less than 50°. Significant work is required to support such observations, so very compelling scientific justification is necessary for approval. See Section 4.1.4 of the Call for Proposals for restrictions on observations of solar system targets, as well as Section 5.3.

2.4 Orientation and Roll Constraints

The orientation (`ORIENT`) of the telescope is defined as the position angle of the U3 axis on the sky measured from north through east (see Figure 2.2).

In principle, *HST* is free to roll about the U1 optical axis. However, this freedom is limited by the need to keep sunlight shining on the solar arrays and by a thermal design that assumes that the Sun always heats the same side of the telescope.

For a particular pointing, the orientation of the telescope that optimizes solar array positioning with respect to the Sun is called the **nominal roll**. At this orientation, the Sun is in the half-plane defined by the U1 axis and the negative U3 axis (see Figure 2.1). Consequently, the nominal roll required for a particular observation depends on the location of the target and date of the observation. The same target observed at different times will, in general, be made at different orientations. Some departures from nominal roll are permitted during *HST* observing (e.g., if a specific orientation is required on a particular date or if the same orientation is required for observations made at different times).

Off-nominal roll is defined as the angle about the U1 axis between a given orientation and the nominal roll. Off-nominal rolls are restricted to less than approximately 5° when the U1-to-sun angle is between 50° and 90°, less than 30° when the angle is between 90° and 178°, and it is unlimited between 178° and 180°. (To achieve an anti-sun pointing of 178° to 180°, the target must lie in or near the plane of the Earth's orbit.)

Observations requiring a certain `ORIENT` for a target at a particular time may not be feasible because the required off-nominal roll angle may be outside the allowed limits. The Visit Planner in the Phase II mode of the Astronomer's Proposal Tool (APT) software can be used in such cases to assess the feasibility of the observations. Please contact help@stsci.edu for assistance.

2.5 Data Storage and Transmission

The Operations and Engineering Division at STScI constructs the *HST* observing schedule, and creates the command loads sent to the telescope. Communications with the spacecraft are performed via the Tracking and Data Relay Satellite System (TDRSS), a network of satellites in geosynchronous orbit. The TDRSS network supports many spacecraft in addition to *HST*. Therefore, the use of the network, either to send commands or receive data from *HST*, must be scheduled. Because of limited onboard command storage capacity and TDRSS availability, the command sequences for *HST* observations are normally uplinked approximately once every eight hours for automatic execution by *HST*. Data are downloaded ten to twenty times per day, depending on the observing schedule.

2.5.1 Onboard Data Storage

HST currently uses large capacity Solid State Recorders (SSRs) to store science data awaiting transmission to the ground. Most *HST* observations are stored on the SSRs and read back to the ground several hours later. Some science programs requiring very high data acquisition rates cannot be accommodated because the instruments would generate more data than either the links or ground system could handle (see Section 6.2.2).

CHAPTER 3:

Telescope Performance

In this chapter...

3.1 Optical Performance

HST's Optical Telescope Assembly (OTA) did not perform as designed because the primary mirror was manufactured with about one-half wave of spherical aberration. This was remedied by corrective optics installed for the science instruments (SIs) during the first servicing mission in December 1993. Since then, all SI detectors (with the exception of the FGSs) have viewed a corrected beam, either via external corrective optics (COSTAR) or via internal optics (for second and third-generation instruments). COSTAR was removed from the telescope during Servicing Mission 4 in May 2009; currently, all onboard instruments have internal corrective optics. Table 3.1 gives a summary of general OTA characteristics.

Table 3.1: HST Optical Characteristics and Performance

Design	Ritchey-Chretien Cassegrain
Aperture	2.4 m
Wavelength Coverage	From 90 nm (MgF_2 limited) to ~3 μm (self-emission limited)
Focal Ratio	*f* /24
Plate Scale (on axis)	3.58 arcsec/mm
PSF FWHM at 5000Å	0.043 arcsec
Encircled Energy within 0.1" at 5000Å	87% (60% - 80% at the detectors)

Because each SI has unique characteristics, the actual encircled energy is instrument-dependent and may vary with observing strategy. The HST Instrument Handbooks (see Section 1.3) should be consulted for instrument-specific point spread function (PSF) characteristics over various wavelength ranges. The Tiny Tim software tool, developed at STScI by John Krist, Tiny Tim webpage with support from Richard Hook at the ST-ECF, can be used to simulate the PSFs of several *HST* instruments. It is available for download from the. PSFs generated by Tiny Tim are coarse matches to observed PSFs because of transient focus changes in *HST* and other effects. As a result, for many types of data analysis, PSF subtraction using Tiny Tim models is inadequate.

3.2 *HST* Guiding Performance

HST's Pointing Control System (PCS) has two guiding modes available. The default guide mode uses Fine Guidance Sensors (FGSs) that maintain high precision pointing control by using guide stars to actively control the telescope pointing. However, the telescope pointing can also be controlled using the rate-sensing gyroscopes.

FGS - Dual Guide Star Acquisitions

The default operational practice is to schedule observations using the Dual Guide Star mode. In a Dual Guide Star Acquisition, two FGSs are used, each locked on a different guide star. The combined pointing information is used to control the pitch, yaw, and roll axes of the telescope. Dual Guide Star Acquisition times are typically six minutes. Reacquisitions following interruptions due to Earth occultations take about four minutes. This pointing control method was designed to keep telescope jitter below 0.007" RMS, which is now routinely achieved. A drift of up to 0.05" may occur over a timescale of 12 hours and more–this is attributed to thermal effects as the spacecraft and FGSs are heated or cooled. As a result, observers planning extended observations in 0.1" or smaller STIS slits should execute a target peak-up maneuver every four orbits (see Section 6.4.2).

FGS - Single Guide Star Acquisitions

In cases where two suitable guide stars are not available, a single guide star acquisition can be used. In this scenario, *HST*'s translational motion is controlled by a guide star in one of the FGSs, while roll motion is controlled by gyros. Therefore, a gyro drift around the guide star will be present that is approximately 1.5 milliarcseconds (mas) of roll angle per second. This introduces a translational drift across the target; the exact size of that drift depends on the roll drift rate, as well as the distance between the single guide star and the instrument aperture (see Figure 2.2). Note, however, that the gyro drift builds up through occultations, typically limiting a visit duration to a few orbits.

There are also occasions when a dual guide star acquisition is planned, but one of the guide stars cannot be acquired. In this case, the Pointing Control System (PCS) will usually carry out the observations using single FGS guiding. A description of this can be found at:

http://www.stsci.edu/hst/observatory/pointing/obslog/OL_7.html

under the header "Single FGS Pitch and Yaw plus Gyro Roll Control" in which a specific application to WFPC2 (a legacy instrument) is discussed. Additional information on single guide star guiding issues, particularly those that require very accurate knowledge of the PSF (including coronagraphic and astrometric programs), or accurate sub-pixel dithering can be found at:

http://www.stsci.edu/hst/acs/faqs/guide_star.html.

The *ACS Instrument Handbook* also contains complementary examples.

Most science programs will not be adversely affected because the drift rates are generally small.

3.3 *HST* Observing Efficiency

HST's "observing efficiency" is defined as the fraction of total time devoted to acquiring guide stars, acquiring astronomical targets, and obtaining the exposure for a target. The main factors that limit the observing efficiency are

- low spacecraft orbit, resulting in frequent Earth occultation of most targets,
- interruptions by passages through the South Atlantic Anomaly,
- the number of user-constrained visits,
- a relatively slow slew rate.

About 90% of the usable observing time is allocated to science observations, with the remainder devoted to calibration and engineering observations (≤10%), and repeats of failed observations (~2%).

CHAPTER 4:

Cycle 25 Scientific Instruments

In this chapter...

4.1 Advanced Camera for Surveys (ACS)

The Advanced Camera for Surveys (**ACS**) was installed during Servicing Mission 3B in March 2002. Failures in the ACS CCD Electronics Box and Low Voltage Power Supply in January 2007 made the WFC and HRC channels inoperable (the SBC continued to function). The problem was partially fixed during Servicing Mission 4 in May 2009, restoring use of the WFC but not the HRC.

In its current state, the camera provides ultraviolet and wide field optical imaging through two channels that have adjacent but not contiguous fields of view. The locations of these channels in the *HST* focal plane are presented in Figure 2.2.

The Wide Field Channel (**ACS/WFC**) provides high throughput and wide field imaging. The camera has a 202" × 202" field of view from 350 nm to 1100 nm. Total system throughput is 42% at 600 nm (see Figure 4.2). The WFC detector is a pair of butted (2K by 4K), thinned and backside-illuminated, SITe CCDs with a red-optimized coating, a long wavelength halo fix, and 15 × 15 μm pixels. The plate scale is 0.050 arcsec/pixel. The WFC PSF is critically sampled at 1160 nm and

undersampled by a factor of three at 370 nm. Well-dithered observations with the WFC should result in a reconstructed PSF FWHM of 0.1" to 0.14".

The Solar Blind Channel (**ACS/SBC**) is optimized for high resolution, solar-blind far-UV imaging. The camera has a 34" × 31" field of view from 115 nm to 170 nm and a peak efficiency of 6% (see Figure 4.2). The detector is a solar-blind CsI Multi-Anode Microchannel detector Array (MAMA) with 25 × 25 μm pixels. The plate scale is 0.032 arcsec/pixel.

The ACS High Resolution Channel (**ACS/HRC**) provided high resolution imaging from Cycle 11 through Cycle 14. This camera is no longer available. More information about the HRC can be found in AppendixC: Legacy Instruments.

In addition to these prime capabilities, ACS also provides imaging polarimetry (Section 4.6.1) and slitless spectroscopy (Section 4.6.2). Further information can be found in the *ACS Instrument Handbook*.

4.2 Wide Field Camera 3 (WFC3)

The Wide Field Camera 3 (**WFC3**) was installed in May 2009 during Servicing Mission 4, replacing the highly accomplished WFPC2. This camera provides ultraviolet, optical, and near-infrared imaging through two independent channels. These channels cannot be operated simultaneously, although they can be operated sequentially within the same orbit. Their location in the *HST* field of view can be seen in Figure 2.2

The Wide Field Ultraviolet-Visible Channel **(WFC3/UVIS)** is a high throughput, panchromatic camera with a field of view of 162" × 162", sensitive to wavelengths from 200 nm to 1000 nm. The total system throughput with this camera is 28% at 600 nm (see Figure 4.2). The detector is a pair of butted, 2K by 4K, thinned and backside-illuminated CCDs with an ultraviolet-optimized anti-reflective coating and 15 × 15 μm pixels. The plate scale is 0.04 arcsec/pixel. In addition to wavelength optimization, the primary differences between the WFC3 and ACS CCDs include a lower read noise (3 e^- for WFC3, 4 e^- for ACS) and a smaller inter-chip gap (465 μm rather than 750 μm). The UVIS channel provides 62 broad-, medium-, and narrow-band filters, and one grism.

The Wide Field High-Throughput Infrared Channel (**WFC3/IR**) has a 136" × 123" field of view over the wavelength range of 800 nm to 1700 nm. The total system throughput with this camera is 50% at 1600 nm (see Figure 4.2). The detector is a 1K by 1K HgCdTe Teledyne array with 18 × 18 μm pixels. The plate scale is 0.13 arcsec/pixel. The detector has 12 e^- RMS read noise in a 16-sample non-destructive readout sequence, or 21 e^- RMS read noise in the difference of two samples (a correlated double sample). The IR channel provides 15 broad-, medium-, and narrow-band filters and two grisms.

WFC3 has slitless imaging spectroscopic modes in both channels and five UVIS quad filters as described in Section 4.6.2.

The "drift and shift" (DASH) method of observations was tested in Cycle 23 and introduced for WFC3/IR GO programs in Cycle 24. It enables users to make large shallow mosaics within one orbit by guiding on gyros alone after the first exposure, thus eliminating the costly overhead of multiple guide star acquisitions. See Section 7.10.6 in the *WFC3 Instrument Handbook*.

The capability of commanding the UVIS shutter to use exclusively one of the two sides of the shutter blade in short exposures, to avoid vibration and PSF smearing, was implemented early in cycle 22. This option (BLADE=A in APT) will be made available to the observer when it is critical to the scientific success of a program. See Section 6.11.4 in the *WFC3 Instrument Handbook*.

Starting in Cycle 20, a major new capability was implement: adding a flash at the end of a UVIS exposure (post-flash). Post-flash greatly increases the detection of faint sources in low background observations where CTE losses would otherwise remove much or all of the flux from those sources. Most UVIS observers should consider using post-flash; it is useful for all UV, narrow-band, and relatively short medium- and broad-band exposures where the detection of faint sources is required. It should replace charge injection in essentially all circumstances. Users considering charge injection rather than post-flash should consult STScI via the help desk. Further information on CTE and post-flash is available in the *WFC3 Instrument Handbook* and at the WFC3 UVIS CTE webpage. Note that, starting in Cycle 23, APT has provided a diagnostic message for UVIS exposures that may have insufficient or excessive flash.

The spatial scanning observing technique was introduced for WFC3 in Cycle 19. This mode can be used to turn stars into well-defined streaks on the detector or to spread a stellar spectrum perpendicular to its dispersion. It is useful for:

- Observations requiring high temporal sampling and/or time resolution.
- More efficient observation and higher S/N observations of exoplanet transits.
- High precision relative astrometric observations.
- Imaging and spectroscopy of brighter sources than previously possible.

See the *WFC3 Instrument Handbook* and WFC3 ISR 2012-08 for further discussion of spatial scanning.

4.3 Fine Guidance Sensor (FGS)

There are three Fine Guidance Sensors (**FGSs**) onboard *HST*. Two FGSs are used to point the telescope at a target and hold that target in the primary scientific instrument's field of view. This task can be performed with a 2 to 5 milliarcsecond pointing stability. The third FGS (FGS1R in Figure 2.2) is used as a sub-milliarcsecond astrometer and a high angular resolution interferometer. This instrument has two operating modes:

- In `POS` (Position) mode, the FGS measures the relative positions of objects in its 69 square arcminute field of view to a precision of ~1 milliarcsecond for targets with magnitudes $3.0 < V < 16.8$. Position mode observing is used to determine relative parallax, proper motion, and reflex motion of single stars and binary systems. Multi-epoch programs have resulted in parallax measurements accurate to 0.2 milliarcsecond or less.
- In the `TRANS` (Transfer) mode, the 5" × 5" instantaneous field of view of the FGS is scanned across an object to obtain an interferogram with high spatial resolution. This is conceptually equivalent to an imaging device that samples an object's PSF with 1 milliarcsecond pixels. The scientific goal of the `TRANS` mode is to study binary star systems (measure the separation, position angle, and relative brightness of the components), as well as to determine the angular size of extended objects such as the disks of resolvable giant stars or asteroids down to ~8 milliarcseconds.

By using a "combined mode" observing strategy, employing both `POS` mode (for parallax, proper motion, and reflex motion) and `TRANS` mode (for determination of visual and relative brightnesses of components in a binary), it is possible to derive the total and fractional masses of binary systems, indicating the mass-luminosity relationship for the components. Additional information can be found in the *FGS Instrument Handbook*.

4.4 Cosmic Origins Spectrograph (COS)

The Cosmic Origins Spectrograph (**COS**) is an ultraviolet spectrograph designed to optimize observations of point sources. It was installed during Servicing Mission 4 in the instrument bay previously occupied by COSTAR. COS is designed to be a very high throughput instrument, providing medium to low resolution ultraviolet spectroscopy. The instrument has two channels for ultraviolet spectroscopy: Far-ultraviolet (FUV) and Near-ultraviolet (NUV).

4.4.1 Far-Ultraviolet Channel (COS/FUV)

COS/FUV uses a single optical element to disperse and focus light onto a crossed-delay-line (XDL) detector; the result is high ultraviolet sensitivity from about 900 Å to 2050 Å with resolving power for different modes ranging from R ~ 1300 to ~ 17,000 (for detailed information on the resolving power of the FUV channel, please see the *COS Instrument Handbook*). This detector has heritage from the FUSE spacecraft. The active front surface of the detector is curved; to achieve the length required to capture the entire projected COS spectrum, two detector segments are placed end-to-end with a small gap between them. Each detector segment has an active area of 85 × 10 mm, digitized to 16384 × 1024 pixels, and a resolution element of 6 × 10 pixels.

The FUV channel has three gratings: G140L provides nearly complete coverage of the FUV wavelength range in a single exposure with a resolving power R ~ 1300 to 3500. G130M spans wavelengths between 900 Å and 1450 Å, and G160M covers the wavelength range between 1400 Å to 1775 Å; both these gratings provide resolving power R between 13,000 and 17,000 for wavelengths longer than 1150 Å (see the next paragraph for resolving power at shorter wavelengths). For all three FUV gratings, a small segment of the spectrum is lost to the gap between the two detector segments. This gap can be filled by obtaining two exposures offset in wavelength.

COS Observations Below 1150 Å

COS observations can be obtained below 1150 Å using either the G140L grating with the 1280 Å setting, or the G130M gratings with the 1055 Å, 1096 Å, or 1222 Å settings.

- G140L Grating with the 1280 Å Setting:
  The G140L/1280 Å setting has R ~ 1300 to 3500 (increasing approximately linearly with wavelength), with a wavelength range from less than 900 Å to 1165 Å (FUVB), with an effective area of 10 cm^2 between 900 Å and 1050 Å, and increasing rapidly to greater than 1000 cm^2 at 1150 Å.
- G130M Grating with the 1055 Å, 1096 Å, and 1222 Å Settings:
  The G130M spectral resolution at the 1055 Å and 1096 Å central wavelength settings has been substantially increased above values offered during previous cycles; they now allow resolutions between 8000 and 10,000 at many wavelengths below 1150 Å. These settings cover the 900 Å to 1236 Å wavelength range with an effective area of approximately 20 cm^2 between 900 Å and 1050 Å. The effective area increases steeply towards longer wavelengths, exceeding 1000 cm^2 by 1150 Å. Users should note, however, that for these modes, the focus values have been set to optimize the resolution over a limited part of their wavelength range (see Figure 4.1).

The resolution values quoted here are based on ray-trace models, so actual resolution may be slightly different. However, preliminary comparison with on-orbit test data appears consistent with the predictions of these models. At the 1055 Å setting, these ray-trace models predict that a resolution between 7000 and 8500 can be obtained on segment B of the COS FUV detector between 900 Å and 970 Å, while for the 1096 Å

setting, resolutions between 7000 and 10,000 can be obtained between 940 Å and 1080 Å. These settings complement the G130M 1222 Å central wavelength setting that was first offered in Cycle 20, which provides resolution of 10,000 to 13,000 between 1067 Å and 1172 Å. At longer wavelengths, the resolution offered by any of these settings will be inferior to that available with the original complement of G130M central wavelength settings (1291 Å, 1300 Å, 1309 Å, 1318 Å, and 1327 Å). Some targets that are too bright to observe at longer wavelengths with the COS G130M grating may be observable on the B segment with the 1055 Å and 1096 Å settings by turning off the A segment which covers the longer wavelengths. However, in this case, there is no usable wavelength calibration lamp spectrum recorded, and the spectrum observed on the B segment cannot be automatically corrected for mechanism drift or zeropoint offsets. For such configurations, GO wavecals have to be inserted following specific rules described in the *COS Instrument Handbook*.

Figure 4.1: Spectral Resolution at LP2 as a Function of Wavelength for the B segment of the COS/FUV Detector with the 1055, 1096, 1222, and 1291 Central Wavelength Settings.

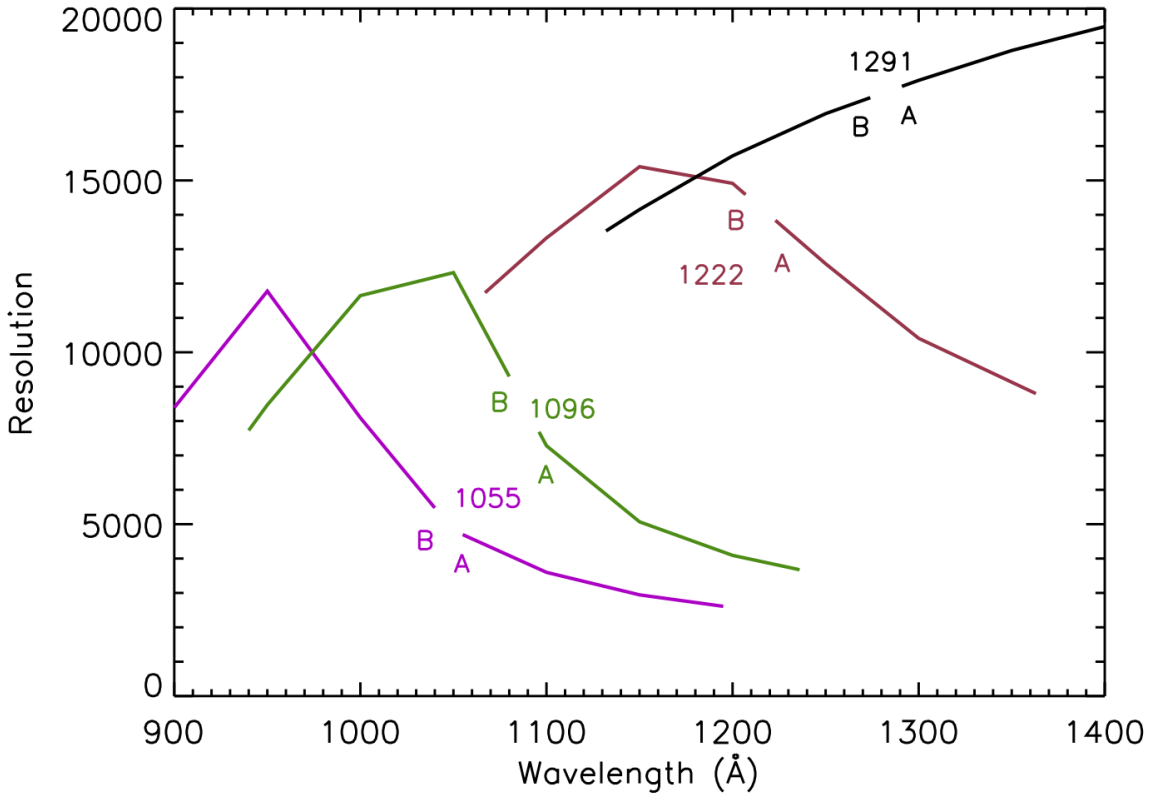

The predicted resolution at LP2 as a function of wavelength for each segment of the COS FUV detector for 1055 Å, 1096 Å, 1222 Å, and 1291 Å central wavelength settings. These predictions are based on ray-trace models. Comparisons with on-orbit results less than 1140 Å are preliminary. The spectral resolution at LP4 is expected to be within 15% of the values shown here. For more detailed information about the spectral resolution at LP4 please see the *COS Instrument Handbook*.

4.4.2 Near-Ultraviolet Channel (NUV)

COS/NUV uses a 1024 × 1024 pixel Cs_2Te MAMA detector that is essentially identical to the STIS/NUV MAMA except that it has a substantially lower dark count. Four gratings may be used for spectroscopy. Portions of the first-order spectra from the gratings are directed onto the detector by three separate flat mirrors. Each mirror produces a single stripe of spectrum on the detector. For the low-dispersion grating, G230L, one or two first-order spectrum stripes are available, each covering ~400 Å of the entire 1700 Å to 3200 Å range at resolving power R ~2100 to 3900, depending upon wavelength. For high-dispersion gratings G185M, G225M, and G285M, three non-contiguous stripes of 35 Å are available in each exposure at resolving powers of 16,000 to 24,000. Panchromatic (1650 Å to 3200 Å) images of small fields (less than two arcseconds) may also be obtained at ~0.06 arcsec or greater resolution in imaging mode.

4.4.3 COS FUV XDL Gain Sag

Prolonged exposure to light causes the COS FUV XDL detectors to become less efficient at photon-to-electron conversion, a phenomenon called “gain sag.” When a particular region of the detector is increasingly used, there is a corresponding decrease in the “pulse height” of the charge cloud generated by an individual photon. As long as the pulse heights are above a minimum threshold needed to distinguish real photons from background events, there is no loss in sensitivity. But as the average pulse height in a particular region approaches and then drops below this threshold, real photon pulses are increasingly misidentified as background, causing a decreasing effective throughput. Since the amount of gain sag increases with the total amount of previous illumination, the effects first appear in regions of the detector that are illuminated by the bright Lyman Alpha airglow line, but eventually, the entire spectrum is affected.

STScI is undertaking a number of actions to mitigate the effects of gain sag and extend the lifetime of the COS FUV XDL detector. On July 23, 2012, the COS FUV spectrum was relocated by 3.5" (about 1 mm) to a part of the detector where significant gain sag had not yet occurred. This move, in conjunction with careful management of the high voltage of the COS FUV detector, has allowed us to obtain data that is free of gain sag artifacts during Cycle 20, Cycle 21 and a fraction of Cycle 22. On February 9, 2015, the COS FUV spectrum was relocated by -6" to another part of the detector at lifetime position 3 (LP3). This LP move along with continued management of the high voltage of the COS FUV detector, has allowed us to obtain data that is free of gain sag artifacts during part of Cycle 22, Cycle 23 and part of Cycle 24. FUV spectra will be moved yet again to a fourth lifetime position (LP4) during Cycle 24 in July 2017 to keep mitigating gain sag effects. The spectral resolution of the COS G130M and G160M gratings at this new position may be 15% lower than at LP3, with a possibly larger resolution decline for the G140L grating.

A new spectral extraction algorithm is used by the COS pipeline to calibrate data obtained at LP3 and will also be used to calibrate data obtained at LP4. This new extraction method is optimized for observations of point sources using the PSA aperture only. FUV spectra of extended sources and FUV spectra obtained with the BOA will be poorly calibrated. As a result, proposers planning to use COS/FUV for science observations with the BOA aperture (whether point source or extended) should carefully consider the impact of the poor calibration on their science goals. See the COS website for updated information on the calibration of the LP4 position.

4.4.4 Optimizing the Science Return of COS

Fixed-pattern noise in the COS detectors limits the signal-to-noise that can be achieved in a single exposure (see Section 5.8 of the *COS Instrument Handbook*). A simple way to remove these detector features is to obtain exposures at multiple FP-POS or CENWAVE settings, both of which shift the spectrum on the detector, and combine them in wavelength space. This is especially important for the COS FUV detector as the fixed pattern noise is larger and more poorly characterized than that of the NUV detector. In addition, the consistent use of multiple FP-POS positions in the G130M and G140L 1105 Å settings will spread the bright geocoronal Lyman Alpha illumination and significantly delay the appearance of gain sag effects.

Since this simple shift-and-add technique significantly improves the signal-to-noise ratio of the resulting spectrum, and will extend the lifetime of the COS FUV detector, the use of multiple FP-POS for each CENWAVE setting is required unless a strong scientific justification to do otherwise is provided in Phase I. This can be achieved by using the FP-POS=ALL parameter in APT for each CENWAVE or by spreading out the four FP-POS positions over multiple orbits within a visit for each CENWAVE or over multiple visits to the same target. Proposers who do not intend to use all four FP-POS for each CENWAVE setting must justify their observing strategy in the Phase I proposals. A modest reduction in observational overheads will not normally be considered sufficient justification for not using all four FP-POS settings. **In addition, in order to continue mitigating the effects of gain sag caused by airglow emission in the FUV B detector, when observing with the G130M grating, STScI reserves the right to switch the G130M central wavelength setting of any program to another G130M central wavelength setting (cenwave). This is to insure that the G130M usage in Cycle 25 is such that a single cenwave is not unreasonably causing the detector to sag. Users that require a specific G130M cenwave must justify it in the phase I.**

COS exposures may be obtained in either a time-tagged photon address (TIME-TAG) mode, in which the position, arrival time, and pulse height (for FUV observations) of each detected photon are saved in an event stream, or in accumulation (ACCUM) mode, in which only the positions of the photon events are recorded. In TIME-TAG mode, which is the default observing mode, the time resolution is 32 milliseconds. ACCUM mode is designed for bright targets with high count rates that would otherwise overwhelm the detector electronics. Because the lower information content of ACCUM

data reduces their utility for archival researchers, its use must be justified for each target. For details, see Section 5.2 of the *COS Instrument Handbook*.

In both TIME-TAG and ACCUM mode, the Astronomer's Proposal Tool (APT) automatically schedules wavelength calibration exposures, either during science exposures or between them (see Section 5.7 of the *COS Instrument Handbook*). The COS data reduction pipeline (CALCOS) uses these data to adjust the zeropoint of the wavelength solution for the extracted spectra. It is possible to suppress the taking of wavelength calibration spectra, but since it significantly lessens the archival quality of COS data, it must be justified.

Observers who wish to employ non-optimal observing techniques must strongly justify their observing strategy in the "Description of Observations" section of their Phase I proposal. Non-optimal observing techniques should not normally be adopted solely for the purpose of producing a modest reduction of the observational overheads; in such cases the observer should normally just request adequate time to use the recommended optimal strategy (see Section 9.2 of the Call for Proposals).

4.5 Space Telescope Imaging Spectrograph (STIS)

The Space Telescope Imaging Spectrograph (**STIS**) was installed aboard *HST* in February 1997. This scientific instrument provides ultraviolet and optical spectroscopy and imaging through three channels. STIS can be used to obtain spatially resolved, long-slit (or slitless) spectroscopy over the 1150 Å to 10,300 Å wavelength range with spectral resolving power from R ~ 500 to 17,500. It can also be used to perform echelle spectroscopy over the 1150 Å - 3100 Å wavelength range at spectral resolving powers of R ~ 30,000 to 114,000, covering broad spectral ranges of $\Delta\lambda$ ~ 800 Å and 200 Å, respectively. STIS can also be used for optical and solar-blind ultraviolet imaging. Three detectors, each with a 1024 × 1024 pixel format, support spectroscopy and imaging as follows:

- The Far Ultraviolet Channel (**STIS/FUV-MAMA**) uses a solar-blind, CsI, Multi-Anode Microchannel detector Array (MAMA), with a field of view of 25" × 25", a plate scale of approximately 0.025 arcsec/pixel, covering the wavelength range from 1150 Å to 1740 Å.
- The Near Ultraviolet Channel (**STIS/NUV-MAMA**) uses a Cs_2Te MAMA detector with the same field of view and plate scale, and covers wavelengths between 1570 Å and 3180 Å.
- The **STIS/CCD** detector, a thinned and backside-illuminated SITe CCD with a coating optimized for the near-ultraviolet, covers the range from 1650 Å to 11,000 Å. This channel's field of view is 52" × 52" and the CCD has a plate scale of 0.05 arcsec/pixel.

The MAMA detectors can be used in ACCUM or TIME-TAG modes, with the latter supporting time-resolutions down to 125 microseconds. The STIS/CCD can be cycled

in ~20 seconds when using small subarrays. The CCD and the MAMAs also provide coronagraphic spectroscopy in the visible and ultraviolet. Coronagraphic CCD imaging is also available. Each of the STIS detectors can also be used for imaging observations, however, only limited filter choices are available.

Summary of STIS changes after SM4

STIS was successfully repaired during Servicing Mission 4. Capabilities are very similar to those prior to the 2004 failure. Overall sensitivities have declined by only a few percent.

However, the STIS CCD has continued to accumulate radiation damage. The mean STIS CCD dark current is estimated to be 0.019 e^-/pixel/s during Cycle 23. Charge transfer efficiency (CTE) declines can also have a strong effect on faint sources observed with the STIS CCD. Users should remember that the STIS ETC does not correct for CTE losses. They can determine the loss due to CTE using the formula described in the *STIS Instrument Handbook* at:

`http://www.stsci.edu/hst/stis/software/analyzing/scripts/cteloss_descrip.html`

CTE effects also produce extended "tails" on hot pixels and cosmic rays that degrade images and spectra, creating an additional source of noise. See STIS ISR 2011-02 for a description of how this can affect STIS CCD data. Use of the E1 aperture positions which place STIS spectra closer to the CCD readout edge will substantially mitigate CTE effects and is strongly recommended for faint targets.

STIS has three newly-supported neutral density filtered slits for use with first order and echelle observations. These three apertures, `31X0.05NDA`, `31X0.05NDB`, and `31X0.05NDC`, provide attenuation factors of 6X, 14X, and 33X, respectively. See the *STIS Instrument Handbook* for more information on the basic properties of these apertures.

There is some evidence that in recent years the STIS instrument focus has changed. Because the STIS corrector mechanism has not been moved since 1997, it is unlikely that the focus will be adjusted unless the performance suffers from additional degradation. The most obvious impact of these focus issues is a decrease in throughput when using apertures smaller than 0.2" in size. This will lower the S/N achieved by an observation of a given length and also reduces the accuracy of the absolute flux calibration. The exact throughput change for a given aperture will vary as the focus changes during the course of HST's normal orbital breathing. Analysis of recent echelle observations taken through the 0.2X0.06 and 0.2X0.09 apertures shows that the average throughput in recent years has been only about 80% of nominal, with occasional individual exposures with these apertures showing as much as a 40% throughput loss. Note that for these apertures, throughput variations of order 10% due to telescope breathing have always been commonly encountered throughout the lifetime of STIS. For the smallest aperture, the 0.1X0.03, average throughput in recent years has typically been only half of its nominal value. Since these throughput losses

vary significantly from observation to observation, it is not possible to simply update the ETC throughputs, as the ETC must also warn against observations which are too bright or which may cause saturation, and must therefore adopt the highest throughput that might reasonably be encountered.

Focus offsets can also affect the relative flux calibration as a function of wavelength within a given observation. For modes covering a wide range of wavelengths, relative flux errors of 10% over the wavelength span of E140M and E230M observations done with the 0.2X0.06 aperture are now common. If combined with small aperture centering errors, these can sometimes increase to as much as 25%. Resolution changes caused by these focus variations appear to be small, although they are measurable in high S/N observations and may affect programs which require extremely high levels of observation-to-observation repeatability.

Users requiring a particular signal-to-noise value when using a small aperture should take these effects into account when estimating the amount of exposure time required. Users requiring absolute or relative flux calibration better than 10% are advised to use apertures of 0.2" wide or larger. For first order observations, the 52X0.5 or 52X2 apertures are recommended to achieve the best photometric results.

After its initial recovery following Servicing Mission 4, the NUV-MAMA showed a much larger dark current than had been previously seen; however, this excess is slowly declining. For planning purposes users should assume that the STIS/NUV-MAMA dark current during Cycle 25 will be 0.0015 counts/pixel/sec. Updated information will be provided as it becomes available. For further details regarding STIS capabilities and for any late breaking updates, see the Cycle 25 *STIS Instrument Handbook* and the STIS website at STScI.

4.6 Additional Observing Modes

4.6.1 Imaging Polarimetry

ACS/WFC provides imaging polarimetry at 0^o, 60^o, and 120^o relative polarization angles. WFC3, STIS and COS do not have polarimetric capability. Please refer to Section 6.1 of the ACS Instrument Handbook for more details.

4.6.2 Slitless Imaging Spectroscopy

Ultraviolet

There are several choices for slitless imaging spectroscopy in the ultraviolet ($\lambda < 3500$ Å). ACS/SBC has two prisms providing R ~ 100 spectroscopy (at 1210 Å) from 1150 Å to 1700 Å. The WFC3/UVIS has a grism for R ~ 70 spectroscopy from 2000 Å to 4000 Å, and the STIS/NUV has a prism covering the range between 1150 Å and 3000 Å with R ~2500. In addition, any first-order STIS mode can be used for

large aperture slitless spectroscopy over a 52" x 52" FOV (STIS CCD gratings) or a 25" x 25" FOV (STIS MAMA first-order gratings.)

Optical

ACS/WFC covers the wavelength range from 5500 Å to 10,500 Å with a grism at R ~100. The STIS CCD also has a number of gratings that can be used for slitless spectroscopy over a 52" x 52" field of view at wavelengths ranging from as short as 1700 Å to as long as 10,200 Å.

Near-infrared

For near-infrared (8000 Å < λ < 25,000 Å) spectroscopy, WFC3/IR has a grism with R ~210 covering wavelengths between 8000 Å and 11,500 Å, and a grism with R ~130 from 11,000 Å to 17,000 Å.

4.6.3 Ramp and Quad Filters

Ramp Filters

ACS has a set of ramp filters covering the wavelength range from 3100 Å to 10,710 Å at 2% and 9% bandwidth. There are five ramp units; each have an inner, middle, and outer segment. The ACS/WFC can use all three segments, providing a total of 15 ramp filters. More information can be found in Section 7.7.2 of the ACS Instrument Handbook.

Quad Filters

WFC3/UVIS contains five quad filters. Each is a 2 x 2 mosaic of filter elements with each quadrant providing a different bandpass for narrow-band line or continuum measurements. Please refer to Section 6.5 of the WFC3 Instrument Handbook for additional information.

4.6.4 Coronagraphy

STIS aperture bars allow for spectroscopic coronagraphy, and the STIS 50CORON aperture provides various wedges and bars that can be used for unfiltered imaging coronagraphy with the STIS CCD. Please refer to Section 12.11 of the STIS Instrument Handbook for additional information. For Cycle 24, the new BAR5 position on the 50CORON aperture location is supported within APT to allow inner working angles as small as 0.25" and with certain observing techniques can reach contrasts as deep as 10^{-6} beyond 0.55". See the STIS BAR5 webpage and the STIS page on coronagraphy with small inner working angles for additional details.

4.6.5 Observations with Two Instruments - Parallel Observing

Observers are encouraged to submit programs that make use of simultaneous observations with two or more cameras. This can greatly increase the scientific value of individual programs and the public Archive. There are two ways to obtain parallel observations: coordinated and pure parallels.

Coordinated Parallels:

As the name implies, coordinated parallel observations allow an observer to use multiple instruments simultaneously in a way that optimizes the telescope pointing (e.g., dither patterns or mosaicing), with exposure and readout times that satisfy the goals of both the primary and parallel science components of a single science program.

Pure Parallels:

Pure parallel observations are proposed independently of any primary GO science program, and are slightly more restrictive in the number of allowed parallel/primary instrument combinations than coordinated parallels. Implementation of pure parallel observing is done by identifying parallel scheduling opportunities that are compatible with primary COS and STIS spectrographic observations for the cycle. Accepted WFC3 and/or ACS pure parallel observations are then matched and structured to schedule simultaneously with those COS and STIS primary observations. Matching and structuring of parallel observations to prime observations, done at the start of the observing cycle, is intended to improve the execution rate for all accepted pure parallel programs.

Policies and Procedures:

The policies for coordinated and pure parallel observing, including allowed instrument usage, are found in the Cycle 25 Call for Proposals.

Detailed descriptions of coordinated and pure parallel observing modes, guidelines for developing a proposal using these modes, and how they are implemented and scheduled, are found in the Parallel Observations User Information Report and the individual instrument handbooks.

4.7 Instrument Comparisons

Hubble Space Telescope observers are presented with several choices of instruments. In many situations, an observer will have to make a selection between complementary cameras, for example, ACS/WFC and WFC3/UVIS, or complementary spectrographs, COS and STIS.

The oldest instruments, STIS and ACS, suffer more severely from CTE losses due to the high radiation environment. The damaging effects of continuous radiation exposure on the CCDs are unavoidable, regardless of whether the camera is operating or not. For STIS, a "Summary of changes after SM4" is available at the end of Section 4.5. For ACS, a summary of CTE considerations is available at the end of Section 4.7.1.

For this cycle, Python Exposure Time Calculators (ETCs) for all instruments are available and can be found at http://etc.stsci.edu/. ETCs use a new computing tool called **PySynphot** (that has replaced the STSDAS **synphot** software package), and has access to the most up-to-date reference files.

As always, please consult the Cycle 25 Announcement webpage for the latest information on the status of HST instrumentation.

4.7.1 *HST* Imaging

ACS, STIS, and WFC3 cameras are available for Cycle 25. Decisions on which camera to use will be made based on wavelength, field of view, spatial resolution, sensitivity, and the availability of specific spectral elements or observing modes. Figures 4.2 to 4.5 provide a set of plots (based on WFC3 SMOV data[1] but still valid for current WFC3 operations) comparing throughput and discovery efficiency for the cameras. Please note that COS/NUV is also available for imaging albeit over a very small field of view. For more information please see Chapter 6 in the COS Instrument Handbook.

In the far-ultraviolet ($\lambda < 2000$ Å) the ACS/SBC is the recommended camera over STIS/FUV-MAMA because it is more sensitive and has a larger number of available filters. For the near-ultraviolet (~2000 Å $< \lambda <$ 3500 Å), WFC3/UVIS is generally recommended over STIS/NUV-MAMA because of its larger field of view and superior sensitivity. Table 4.1 contains a detailed comparison between WFC3/UVIS and STIS/NUV-MAMA.

1. For IR throughputs, please refer to WFC3 ISR 2009-30 and WFC3 ISR 2011-08. For UVIS throughputs, WFC3 ISR 2009-31 and WFC3 ISR 2010-14.

Table 4.1: Imaging at Near-UV Wavelengths (200 nm - 350 nm)

	WFC3/UVIS	STIS/NUV-MAMA
FOV area (arcsec^2)	162" x 162" (26,183)	25" x 25" (625)
Broad-band throughput @ 230, 330 nm	0.08, 0.19	0.026, 0.002
Pixel scale (arcsec)	0.040	0.025
Number of pixels	4k x 4k	1k x 1k
Read noise (e^-)	3.1	None
Dark current	7 (e^-/pix/hr)	5.4 (cts/pix/hr)
Number of filters	13	9
Number of full-field filters	10	8 (2 ND)
Number of quad filters	3	1 ND

WFC3/UVIS has the highest throughput among *HST* imaging instruments in the wavelength range extending from its blue cut-off (at 200 nm) to ~400 nm. Beyond that wavelength range, the choice of which *HST* instrument is best suited for observations depends on the specific requirements of the science program.

Although the absolute throughput of ACS is higher at optical wavelengths, the excellent WFC3/UVIS efficiency in the range of 400 nm to 700 nm, coupled with its 20% smaller pixels, 25% lower read noise, relatively small CTE corrections, and much lower dark current can make it the preferred instrument in some cases of optical imaging. Alternately, the 50% larger ACS/WFC field of view or the availability of imaging polarizers can be considerations potentially important for users. The optimal choice between the two instruments may require careful predictions from their respective ETCs, factoring in detailed observational setup. Table 4.2 presents a detailed comparison between WFC3/UVIS and ACS/WFC.

Table 4.2: Imaging at Optical Wavelengths (350 nm - 1000 nm).

	WFC3/UVIS	ACS/WFC
FOV area (arcsec^2)	162" x 162" (26,183)	202" x 202" (40,804)
Broad-band throughput[1] @ B,V, I, z	0.23,0.28, 0.16, 0.09	0.34,0.41, 0.36, 0.20
Pixel scale (arcsec)	0.040	0.049
Number of pixels	4k x 4k	4k x 4k
Read noise (e^-)	3.1	4
Dark current (e^-/pix/hr)	7	22
Number of filters	49	27
Number of full-field filters	32	12
Number of quad filters	17	15
Number of polarizers	0	6

1. Average throughput at 10 nm bandpass at the pivot wavelength (B = F438W, V = F606W, I = F814W, z = F850LP).

In the near-infrared (8000 Å < λ < 25,000 Å) the WFC3/IR has superior throughput and a much larger field of view than the now-defunct NICMOS. The data obtained with WFC3/IR should be easier to reduce and calibrate due to accurate bias subtraction made possible by the presence of reference pixels. WFC3/IR is currently the only option to perform near-infrared observations with *HST* since NICMOS is no longer available. For reference purposes, Table 4.3 provides a comparison between WFC3/IR and three NICMOS channels.

Table 4.3: Imaging at Near-Infrared Wavelengths (800 nm - 2500 nm).

	WFC3/IR	NIC3	NIC2	NIC1
FOV area (arcsec^2)	123" x 136" (16,728)	51" x 51" (2601)	19" x 19" (361)	11" x 11" (121)
Broad-band throughput @ 1.1, 1.6 μm	0.49, 0.50	0.13, 0.20	0.14, 0.20	0.12, 0.18
Wavelength range (μm)	0.9- 1.7	0.8 - 2.5	0.8 - 2.5	0.8 - 1.8
Pixel scale (arcsec)	0.13	0.200	0.075	0.043
Number of pixels	1014 x 1014	256 x 256	256 x 256	256 x 256
Read noise, CDS (e^-)	21	29	26	26
Number of filters Number of polarizers	15 0	16 0	16 3	16 3

The following four figures present a graphical comparison of the *HST* imaging detectors with respect to several useful parameters: system throughput, discovery efficiency, limiting magnitude, and extended source survey time.

System throughputs as a function of wavelength are shown in Figure 4.2. The plotted quantities are end-to-end throughputs, including filter transmissions calculated at the pivot wavelength of each broad-band filter.

Figure 4.2: *HST* Total System Throughputs

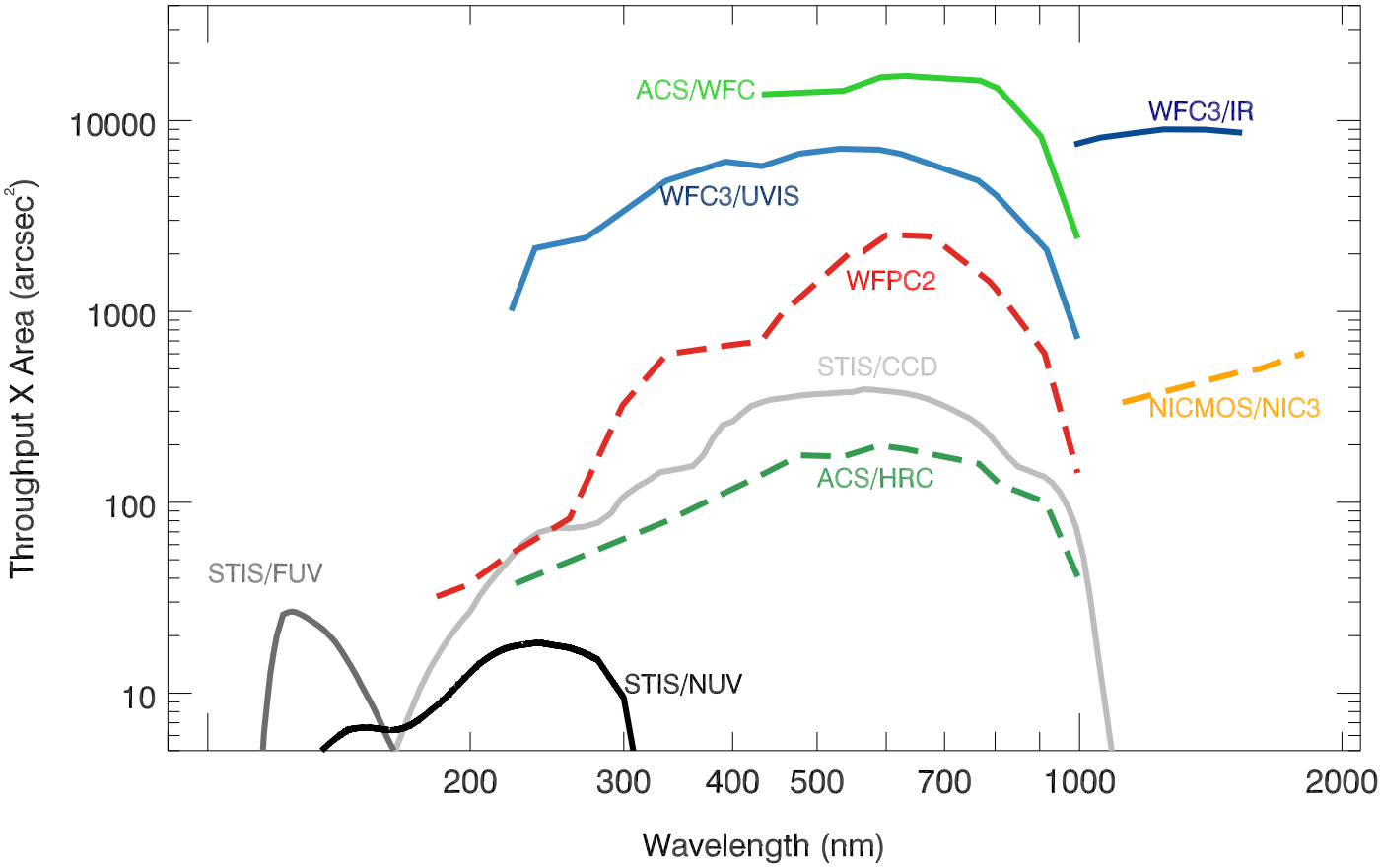

Full lines represent instruments that will be offered during Cycle 25. Dashed lines represent instruments that are not available for Cycle 25 (HRC, NICMOS) and a previously flown instrument (WFPC2).

Discovery efficiencies of the cameras, defined as the system throughput multiplied by the field of view area, are shown in Figure 4.3.

Figure 4.3: *HST* Survey Discovery Efficiencies

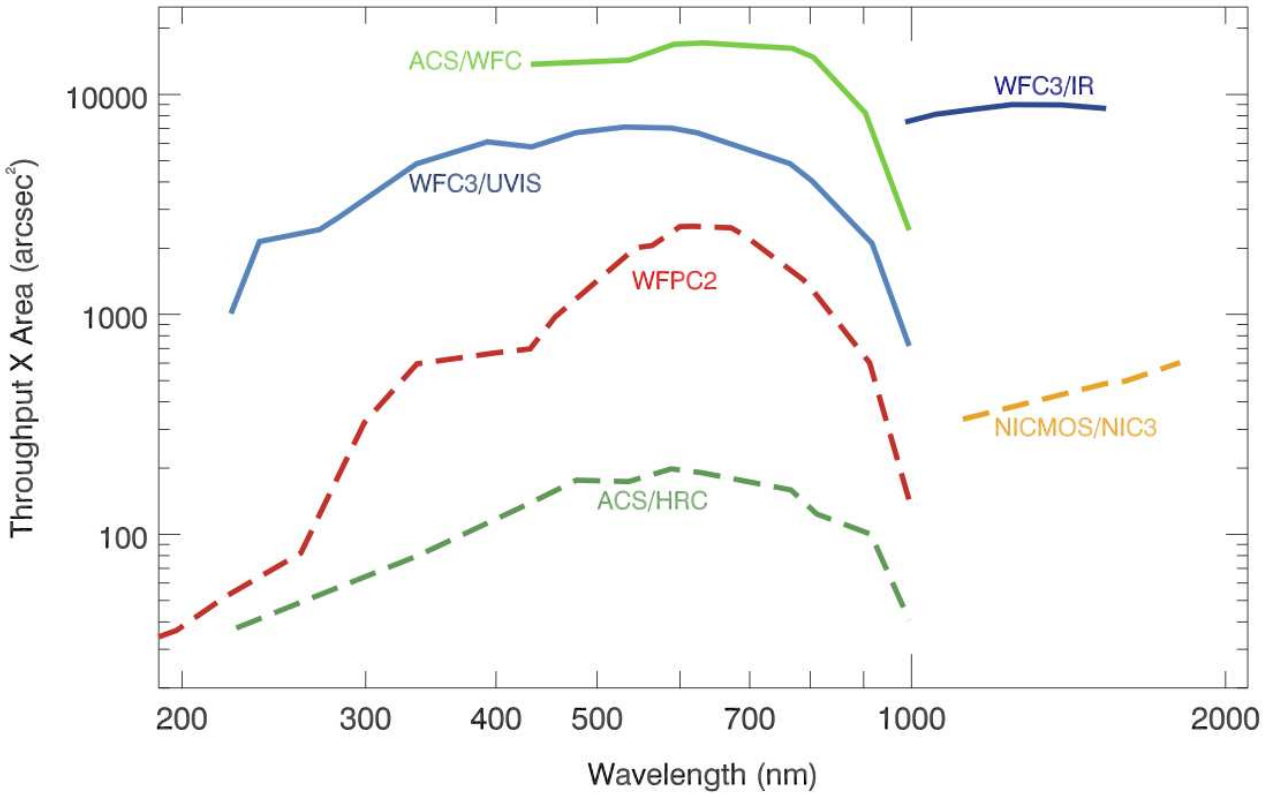

Full lines represent instruments that will be offered during Cycle 25. Dashed lines represent instruments that are not available for Cycle 25 (HRC, NICMOS) and a previously flown instrument (WFPC2).

The point source limiting magnitude achieved with a signal-to-noise of 5 in a 10 hour exposure time with optimal extraction is shown in Figure 4.4.

Figure 4.4: Point-Source Limiting Magnitude

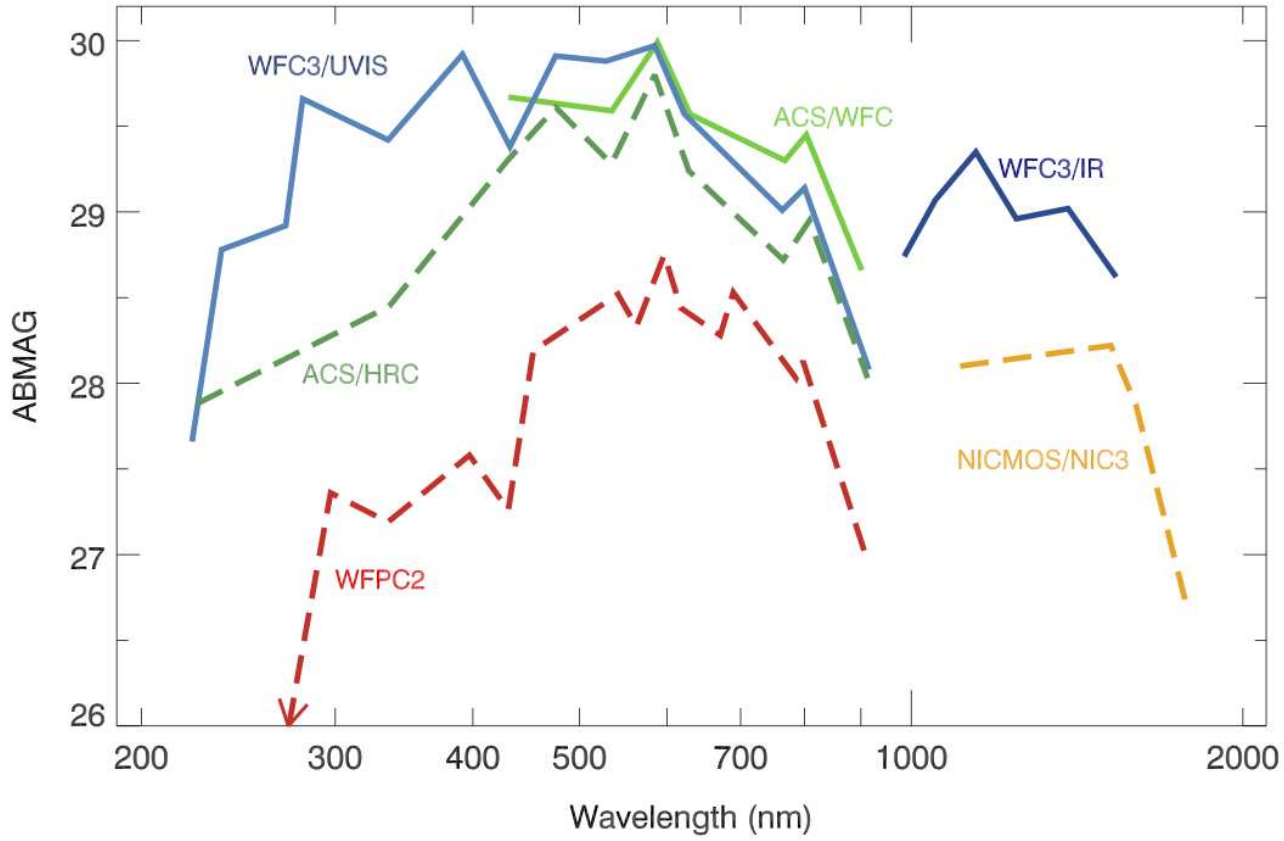

Full lines represent instruments that will be offered during Cycle 25. Dashed lines represent instruments that are not available for Cycle 25 (HRC, NICMOS) and a previously flown instrument (WFPC2).

Figure 4.5 shows the extended source survey time to attain ABMAG = 26 mag in an area of 100 arcmin^2.

Figure 4.5: Extended-Source Survey Time

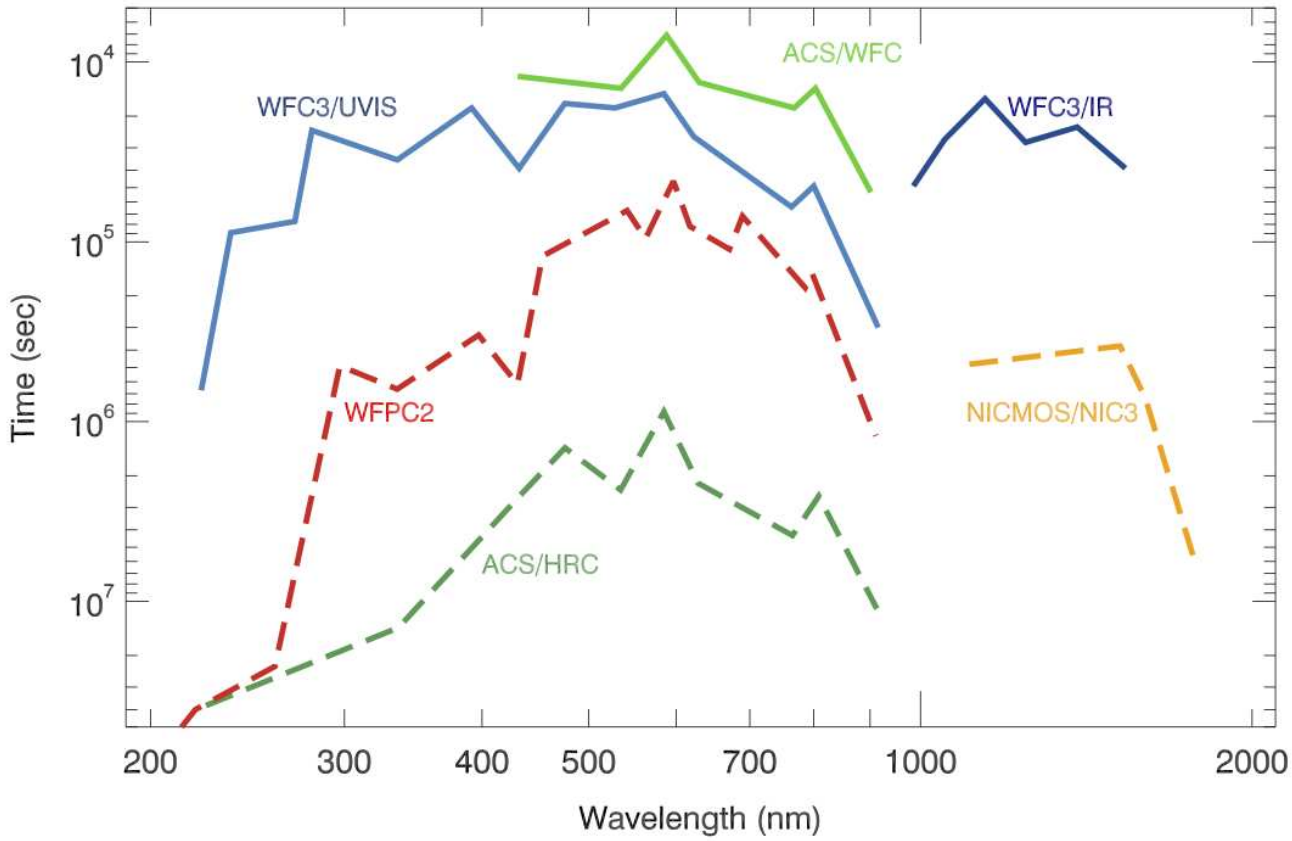

Full lines represent instruments that will be offered in Cycle 25. Dashed lines represent instruments that are not available for Cycle 25 (HRC, NICMOS, and WFPC2).

CTE for ACS/WFC has degraded significantly since it was installed aboard HST in 2002. The charge-trailing caused by poor CTE during ACS/WFC readout can be reduced by positioning a target close to one of the serial registers (e.g.: aperture location 'WFC1-CTE'), or by increasing the image background either naturally (e.g.: longer exposure time; broader filter bandpass) or artificially (using LED post-flash). Much effort, both internal and external to the ACS Team, has gone into minimizing the science impact from ACS/WFC charge transfer inefficiency.

The ACS Team has developed a pixel-based CTE correction technique, described by Anderson & Bedin (2010, PASP, 122, 1035), for post-readout deconvolution of charge-trailing. This correction is applicable to ACS/WFC full-frame readouts, to 2K-subarray readouts, and from Cycle 24 onwards, to the smaller subarray readouts. The CALACS pipeline generates both CTE-corrected (FLC/DRC) and

CTE-uncorrected (FLT/DRZ) reductions of WFC imagery for full-frame images; for subarray images, the pixel-based CTE correction is available as a stand-alone code in the 'acstools' software suite. Please consult the ACS webpage for the latest details.

4.7.2 Spectrographs

For observations requiring resolutions of R > 15,000, COS is more sensitive than STIS by factors of 10 to 30 in the far-ultraviolet (~1150 Å < l < 2050 Å) and by factors of two to three in the near-ultraviolet (~1700 Å < l < 3200 Å) for some NUV gratings (see *COS Instrument Handbook*). COS also has a unique but limited capability to observe wavelengths between 900 Å and 1150 Å. However, it does not operate in the optical. Please refer to the *COS Instrument Handbook* for important factors concerning COS observations in this wavelength range.

COS is optimized for observing faint point source targets, making it the instrument of choice for such objects. COS has an aperture of 2.5" in diameter. COS/FUV spatial resolution is limited to 1", while COS/NUV spatial resolution is approximately 0.06". However, for sources larger than approximately 1" perpendicular to the dispersion direction, portions of the spectrum may overlap on the NUV detector. Therefore, when spatial resolution is required, STIS is usually the preferred instrument. STIS first order NUV and FUV MAMA modes have a spatial resolution of about 0.05" over a 25" long slit, while STIS CCD spectral modes (1900 Å - 10,200 Å) have a spatial resolution of about 0.1" with a 52" long slit.

STIS high dispersion echelle modes have significantly higher spectral resolution than COS (R ~100,000 vs. R ~20,000), which is essential for some science programs. In addition, the STIS/NUV medium resolution echelle mode, E230M, has a wider wavelength coverage in a single exposure (~800 Å) than does a single COS/NUV medium resolution exposure (100 Å to 120 Å in three discontinuous pieces). Despite the sensitivity advantage of COS in the NUV, when complete coverage of a broad wavelength range is needed, STIS is the more efficient choice. In particular, the sensitivity of the COS/G285M configuration is no longer better than that of STIS configurations of comparable spectral resolution and covering similar wavelength ranges. STIS also has a wider variety of apertures than COS; this includes a number of neutral density apertures that makes STIS the preferred instrument for many UV bright objects. Given the low usage of most COS/NUV modes, it is likely that calibrations for comparable STIS/NUV modes will be more robust.

A useful comparison of COS and STIS at ultraviolet wavelengths is given in Table 4.4.

Table 4.4: Spectroscopy at Ultraviolet Wavelengths

		COS/FUV	COS/NUV	STIS/FUV	STIS/NUV
Spectral coverage (Å)		900 - 1775 (M) 900 - 2050 (L)	1700 - 3200 (M) 1650 - 3200 (L)	1150 - 1700 ---	1650 - 3100 ---
Effective area (cm^2)					
950 Å (FUV)		20 (G130M)	---	---	---
1300 Å (FUV)		3000 (M)	600 (M)	400 (M)	350 (M)
2500 Å (NUV)		1800 (L)	750 (L)	1700 (L)	900 (L)
Resolving	H	---	---	114,000	114,000
power	M	16,000 - 17,000	16,000 - 24,000	11,500 - 45,800	9100 - 30,000
$R = \lambda/d\lambda$	M ($\lambda < 1150$)	13,000 & 1000 - 3000	---	---	---
	L	1500 - 4000	2100 - 3200	1000	500 - 1005
Number of pixels along dispersion		16,384[1](32,768)[1]	1024	1024 (2048)	1024 (2048)
Background [2] (counts/sec/resel)		2.40×10^{-4} (FUVA) 2.38×10^{-4} (FUVB)	7.74×10^{-3}	1.5×10^{-3}	9.0×10^{-3}
Background Equivalent Flux (ergs/cm^2/sec/Å)		7.6×10^{-17} G130M at 1264 Å	4.8×10^{-15} G225M at 2160 Å	9.0×10^{-15} E140M at 1297.5 Å	8.0×10^{-15} E230M at 2581 Å

1. The first number is number of pixels along the dispersion per segment; the second number is for both segments
2. One resel is considered 6x10 pixels for COS/FUV, 3x3 pixels for COS/NUV, 2x5 pixels for STIS/FUV, and 2x3 pixels for STIS/NUV.

The throughputs of COS and STIS in the ultraviolet, including the effect of the *HST* OTA, are shown in Figure 4.6. STIS throughputs do not include slit losses. The effective area of COS modes below 1150 Å is shown in Figure 4.7. This figure has not been updated for recent throughput changes. For an optimal evaluation of the choice of COS vs STIS, the exposure time calculators (ETCs) should be used.

Figure 4.6: Throughputs for COS and STIS in the FUV and NUV.

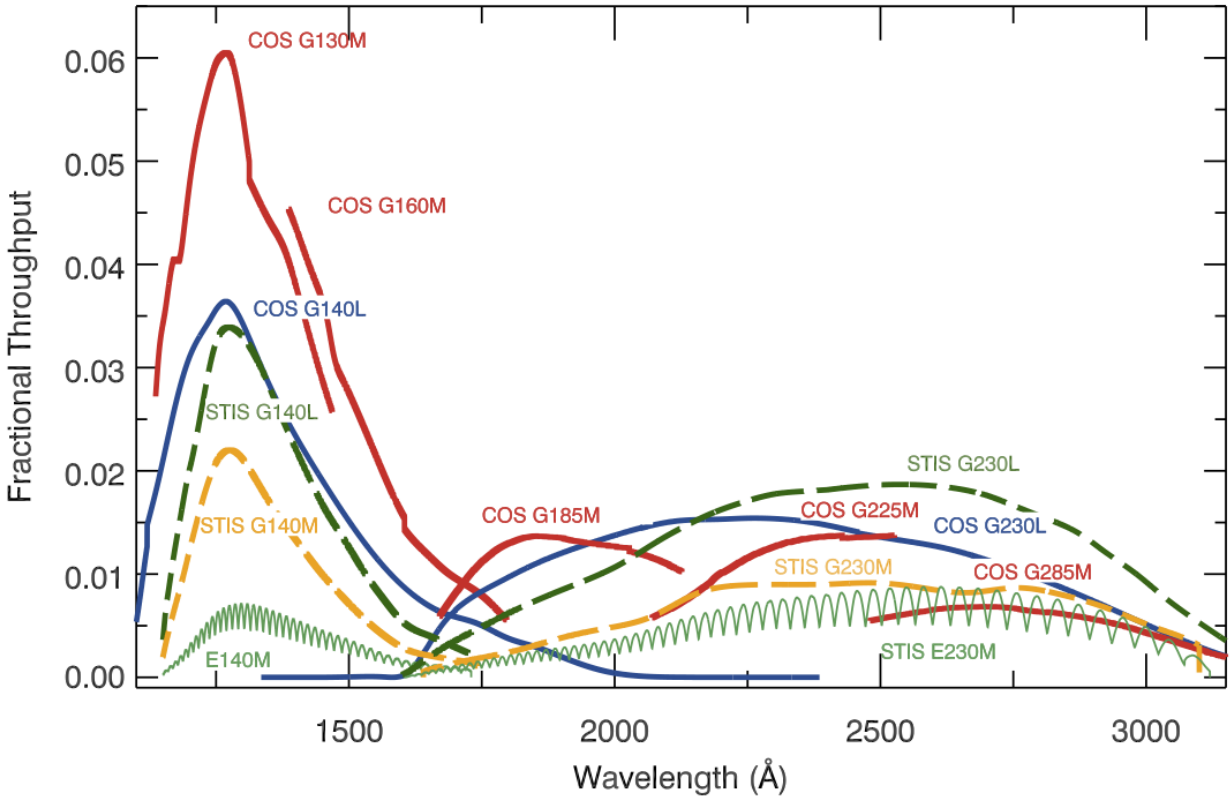

Figure 4.7: Effective Area for COS Below 1150 Å

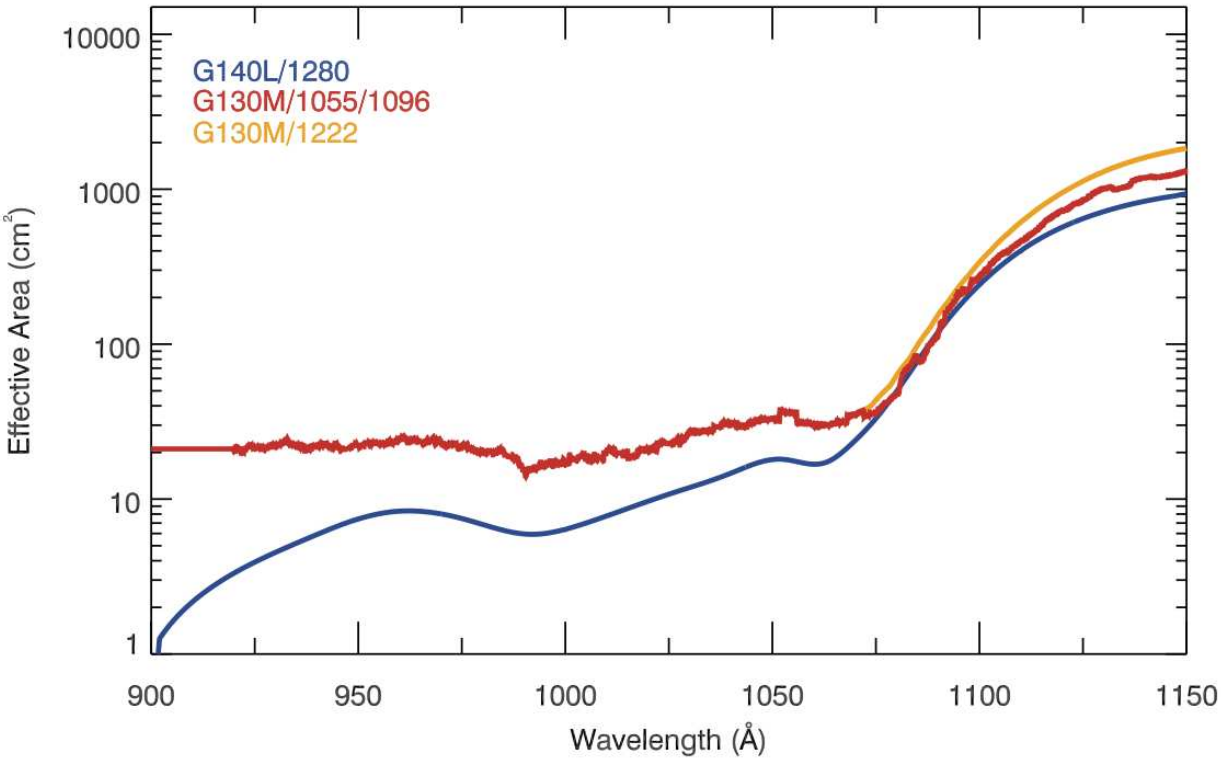

A comparison of the effective area of the G130M modes (red) with that of G140L (blue). The G130M effective area below 920 Å is not well characterized, so the value at 920 Å is used to extrapolate to shorter wavelengths, shown in yellow. The new mode (G130M/1222 Å) is also shown.

CHAPTER 5:

Observing Considerations

In this chapter...

5.1 Bright-Object Constraints

Some scientific instruments must be protected against over-illumination. Observations that violate these protections cannot be executed and should not be proposed. The constraints discussed below are *safety* constraints.

Data may also be affected by bright objects at limits that are substantially fainter than the safety limits discussed in the following sections. Such bright object-related effects include non-linearity, saturation, and residual image effects. Please consult the relevant HST Instrument Handbooks (see Section 1.3) for details.

5.1.1 ACS, COS & STIS

ACS and STIS CCDs have no safety-related brightness limits.

The MAMA detectors in the ACS/SBC, COS (NUV), and STIS, as well as the COS/XDL (FUV) detector, can be damaged by excessive levels of illumination and are therefore protected by hardware safety mechanisms. In order to avoid triggering their safety mechanisms, successful proposers using these detectors are required to perform a detailed check of the field surrounding their targets for excessively bright

sources (this must be done by the Phase II deadline). Bright object checks can be done using tools in APT. Exceptions to Phase II bright object checks are moving targets; these must be cleared after scheduling windows have been established. Due to the complexity of bright object checks for moving targets, no further changes to the observing setup are permitted once such targets have been cleared.

Bright object count rate limits are mode dependent. Specific values are given in the instrument handbooks, including example magnitude screening limits for astronomical objects observed in the most commonly used modes. In addition, the Exposure Time Calculators (ETCs), accessible from the HST Instruments webpage, can be used to determine if a particular target and instrument configuration combination exceeds the global or local count rate screening limits.

Objects with strong UV fluxes (e.g., early-type stars) can have a screening limit as faint as V = 19. Therefore, proposers using any of these health and safety instrument modes must refer to the relevant instrument handbooks for instructions on performing a detailed analysis for their specific sources, and discuss the results in the Description of the Observations section of the Phase I proposal (see Section 9.2 of the Call for Proposals). Both the targets and other objects in the FOV will have to be cleared during Phase II, but if the field is particularly crowded or if any object in the FOV is known to pose a brightness concern, observers are asked to explain, in the "Description of Observations" section of the Phase I program, how they propose to clear them during Phase II.

For the STIS MAMAs, these limits are given in Section 7.7 of the *STIS Instrument Handbook*. For the COS XDL and MAMA, screening limits are given in Chapter 10 of the *COS Instrument Handbook*. For the SBC, the V magnitude screening limits are quoted in Section 7.2 of the *ACS Instrument Handbook*. Note that for SBC prism spectroscopy, a direct image must be added manually to provide the wavelength calibration, and it will drive the safety issue since the direct filters are more sensitive than the prisms. This image must be included in the Observing Summary (see Section 8.15 of the Call for Proposals) and the safety discussion.

In the case of irregular variables that are either known to undergo unpredictable outbursts, or belong to classes of objects that are subject to outbursts, the proposer must determine whether the target will violate the bright object limits during outburst. If a violation is possible, the proposer must outline a strategy that will ensure that the target is safe to observe with COS, STIS/MAMA or ACS/SBC. The observing strategy might include additional observations, obtained over a timescale appropriate to the particular type of variable object, with either *HST* or ground-based telescopes. If *HST* data are to be used for this purpose, the required orbits must be requested in Phase I (see Section 4.1.3 of the Call for Proposals). STScI reserves the right to limit the number of visits requiring quiescence verification observations within 20 days or less of an HST observation to no more than 12 such visits per Cycle. Further details about these procedures are presented in ACS ISR 06-04. The general policies described there apply to the STIS/MAMA and COS detectors as well, with suitable scaling for the differences in the exact Bright Object Protection (BOP) limits for each detector and mode. These limits are described in the individual instrument handbooks.

5.1.2 FGS

Objects as bright as V = 3.0 may be observed if the 5-magnitude neutral-density filter (F5ND) is used. Observations of all objects brighter than V = 8.0 should be performed with this filter. A hardware limitation prevents the FGS target acquisition from succeeding for any target brighter than V = 8.0 (3.0 with F5ND.)

5.1.3 WFC3

There are no safety-related brightness limits for WFC3. Furthermore, overexposure of UVIS images does not leave persistent signals in subsequent exposures. Signals in IR images that are greater than approximately half full well do persist and have significant implications for design of observing strategies and data analysis. See the *WFC3 Instrument Handbook* for more information.

5.2 Target Acquisitions

Target acquisition is the procedure used to ensure that the target is in the field of view of the requested aperture to the level of accuracy required by the observer. There are several distinct methods of target acquisition; each method has a different approach and different accuracy and will take different amounts of time and resources to complete. The required level of accuracy depends on the size of the aperture used to obtain the science data and on the nature of the science program.

5.2.1 Target Acquisition without the Ground System

Blind acquisition

For blind acquisition, guide stars are acquired and the FGSs are used for pointing control. The pointing is accurate to the guide star position uncertainty, which is approximately 0.3" RMS, plus the instrument-to-FGS alignment error.

Onboard acquisition

For onboard acquisition, software specific to the scientific instrument centers the fiducial point onto the target. Onboard target acquisitions are needed for COS and STIS spectroscopic observations (except slitless) and all coronagraphic observations with STIS. WFC3 does not have onboard acquisition capabilities, which means that all WFC3 target acquisitions are blind acquisitions. For specific information on methods and expected pointing accuracies, see the HST Instrument Handbooks.

Early acquisition

For early acquisition, an image is taken in an earlier visit and analyzed by the PI. The PI may then update the target coordinates in the Phase II proposal for use with subsequent visits.

5.2.2 Target Acquisition with Ground System Support

Target acquisitions that cannot be accomplished successfully or efficiently via one of the above mentioned methods may still be possible with STScI ground system support. This is accomplished by analyzing certain data, calculating and uplinking appropriate pointing corrections to the telescope.

One example is a technique to avoid repeating multistage target acquisitions for an object that will be observed in several visits with the same instrument configuration, using the same guide stars. Multistage target acquisitions to center a target in a small aperture (as in STIS) consume a large fraction of orbital visibility in an orbit. However, if the offsets are determined from engineering and image data obtained from the initial successful target acquisition, those offsets can then be applied to subsequent visits. Request for this support is implicit in the specification of the "Save Offset" and "Use Offset" special requirements in the Phase II proposal.

5.3 Solar System Targets

Objects within the Solar System move with respect to the fixed stars. *HST* has the capability to point at, and track moving targets, including planets, their satellites and surface features on them, with sub-arcsecond accuracy. However, there are a variety of practical limitations on the use of these capabilities that must be considered before addressing the feasibility of any particular investigation. Proposals to observe the Moon, for example, will be permitted in Cycle 25. Please consult the Lunar Observations User Information Report (UIR-2007-01) for more information.

HST is capable of tracking moving targets with the same precision achieved for fixed targets. This is accomplished by maintaining FGS Fine Lock on guide stars, and driving the FGS star sensors in the appropriate path, thus moving the telescope to track the target. Tracking under FGS control is technically possible for apparent target motions up to 5 arcsec/s. In practice, however, FGS tracking of a fast moving target may be able to accommodate a full HST orbit's worth of observing even if the target motion forces the guide stars out of the FGS apertures before completion of the orbit; in such cases, it is possible to continue observing under (less accurate) gyro guiding.

The track for a moving target is derived from its orbital elements. Orbital elements for all planets and their satellites are available at STScI. For other objects, the Principal Investigator (PI) must provide orbital elements for the target in the Phase II proposal. The "Requires Ephemeris Correction" special requirement, described in the Phase II Proposal Instructions can be used to insert an offset shortly before the observation is executed to eliminate "zeropoint" errors due to an inaccurate ephemeris. See Section 4.1.4 of the Call for Proposals for restrictions on observations of Solar System targets.

5.4 Offsets, Patterns, and Dithering

Offsets are routinely used to reposition a target in the instrument field of view. The size of the offset is limited by the requirement that both guide stars remain within the respective fields of view of their FGSs. Offsets within single detectors (the most common type) can be performed to within ±0.003". Offsets that continue across separate visits (when executed with the same guide stars) will typically have an accuracy of ~0.05".

Patterns are used to place the telescope at multiple positions to allow for dithered or mosaiced observations. Patterns can define a linear, spiral, or parallelogram series of observation points. Patterns can also be combined to produce a more complex series of observation points. In addition, "convenience patterns" have been predefined to represent typical dither and mosaic strategies; for details see the Phase II Instructions available at the Phase II Program Preparation webpage. The possible pattern area is limited by the requirement that the same guide stars be used throughout the pattern. This implies a maximum of about 120 arcseconds of linear motion.

For most small- or medium-sized imaging programs (i.e., up to a few orbits per target/field combination), dither patterns are designed to provide half-pixel subsampling, and to move bad pixels and inter-chip gaps to different locations on the sky. Larger programs may benefit from more complex dithering strategies, to provide, for example, even finer subsampling of the detector pixels. The data can be combined using the DrizzlePac software provided as part of PyRAF/STSDAS. More details are provided in the *DrizzlePac Handbook*.

In general, undithered observations with the ACS CCDs, and WFC3's CCD and IR detectors, will not be approved without strong justification for why it is *required* for the scientific objectives. Otherwise, hot pixels and other detector artifacts will compromise the program and the archival value of the data. Further details about the options and advantages of ACS patterns can be found in the *ACS Instrument Handbook*, the Phase II Proposal Instructions, and the ACS Dither webpage. Information on dithering for WFC3 observations is found in Appendix C of the *WFC3 Instrument Handbook*, the Phase II Proposal Instructions, and WFC3 ISR 2010-09.

STIS CCD observations may normally benefit from dithering to eliminate hot pixels and improve PSF sampling, although for spectroscopic observations, this may complicate data reduction. See the *STIS Instrument Handbook* and the Phase II Proposal Instructions for further details.

5.5 Spatial Scans

Spatial scan capability, available only for WFC3, facilitates cutting edge photometric and astrometric observations of very bright targets. This mode supports observations that otherwise would result in detector saturation, and it provides the potential to expand the use of WFC3 to new areas of scientific discovery. For some science applications, this mode can also result in greater scientific return using fewer *HST* orbits.

The use of spatial scans is not permitted with coordinated or pure parallels, moving targets, and internal targets. Additionally, scan exposures may not use the optional parameter `CR-SPLIT` and may not have special requirements that force them to occur at the same spacecraft position as another exposure. Please see the Phase II Proposal Instructions, the *WFC3 Instrument Handbook* and WFC3 ISR 2012-08 for more details on this mode.

CHAPTER 6:

Orbit Calculation for a Phase I Proposal

In this chapter...

6.1 Overview of an Observing Program

6.1.1 General Observer (GO) Programs

Definitions (*HST* Orbits, Orbital Visibility Periods, and Visits)

HST GO observing time is counted in terms of *orbits*. Each 96-minute orbit contains a certain amount of useful time when the target can be observed, called the *orbital visibility period.* The length and timing of the visibility period depends on the declination of the target and on whether there are any special scheduling constraints. Orbits are grouped into larger units called *visits*; a visit is a series of one or more exposures on a target, including overheads, that will execute in one or more consecutive orbits.

Components of a Visit

The orbits in a visit generally contain the following components:

- Guide star acquisition and re-acquisition of a target is required to ensure that *HST* can maintain adequate pointing during each orbit. Guide star acquisition is needed for the first orbit in a visit, and re-acquisition is needed for subsequent orbits in that same visit. See Section 3.2 for details on telescope guiding.

- Target acquisition is needed if the target must be placed in an instrument aperture. Imaging observations (unless they are coronagraphic) generally do not require a target acquisition. See Section 5.2 for details on target acquisition strategies.
- The science exposures.
- Instrument overheads (e.g., the time required to set up the instrument and read out the data).
- Telescope repositioning overheads for small angle maneuvers such as pattern dithers and offsets.
- Special calibration observations which may be required if the accuracy provided by the standard calibrations is inadequate for the goals of the project (see Section 4.3 of the Call for Proposals).

Preparing a Phase I Program

Use the following steps to calculate the resources required for a GO program:

1. Define the observations (instrument set-up, number of exposures, exposure times, etc.) for each target. Use the instrument handbooks at the HST Instruments webpages and the Exposure Time Calculator (ETC) tools as primary resources.
2. Group observations into separate visits following the guidelines in Section 6.2.
3. Determine the orbital visibility period of each target in the proposal (described in Section 6.3). Programs requesting 75 or more orbits in a single cycle must use the visibility periods listed in Table 6.1. For LARGE programs, these visibility periods will be enforced for approved programs in Phase II.
4. Compute the times required for guide star acquisitions, target acquisitions, instrument overheads, and telescope repositioning overheads (described in Section 6.4 and Appendix A). See Section 3.2.3 of the Call for Proposals.
5. Lay out all the exposure and overhead times for the program into visits (described in Section 6.5) and add up the number of orbits from each visit to obtain the total orbit request. Each visit must consist of an integer number of orbits. Partial orbits are not granted.

6.1.2 Snapshot Programs

In a Phase I Snapshot proposal, the PI specifies a requested number of targets, rather than a requested number of orbits. The exposure times and overhead times for Snapshot observations are calculated in similar fashion as for GO observations. *The observations for a Snapshot target, including all overheads and the final data dump, are typically 45 minutes or less*. See UIR-2014-001 for guidance on orbit length.

See Section 3.3 of the Call for Proposals for detailed policies and procedures for Snapshot observations.

6.2 *HST* Visits

6.2.1 Defining New Visits and Optimizing Scheduling Efficiency and Flexibility

Guidelines and Rules

The following recommended guidelines were put in place to ensure scheduling efficiency and flexibility, and to maximize the number of scheduling opportunities during the *HST* observing cycle:

1. For health and safety reasons, observations using the STIS MAMAs and ACS/SBC should not exceed five orbits.
2. Exposures should be ordered and grouped such that instrument overheads occur between orbital visibility periods in multi-orbit visits.
3. Changes in *HST* pointing within an orbit should not exceed ~2 arcminutes. This can be due to an explicit change in target position (e.g., POS TARG, dither pattern, aperture change) or the use of a new target. *Changes larger than 2 arcminutes introduce major slews which may be accommodated only if science goals dictate and conditions allow it*.

A new visit is ***required*** if any of the following conditions occur:

1. A change in HST pointing of greater than ~1°.
2. The interval of time between repeated or periodic exposures creates an empty orbital visibility period (an orbit with no exposures).
3. There is a required change in telescope orientation between observations (e.g., for STIS long-slit spectra along different position angles on the sky).

A more complete explanation of the rationale behind these guidelines and rules can be found at:

http://www.stsci.edu/hst/programs/recommendations

The practical implementation of these guidelines is dictated by the details of the telescope and instrument operating characteristics. Proposers should use the Phase I documentation and proposal tools to gain insight into how well a proposed observing scenario satisfies each of the guidelines.

In general, the rule of thumb is that "smaller is better." Thus, smaller visit durations, target separations, and instrument configurations are better, where "better" refers to telescope scheduling efficiency and flexibility. STScI will work with observers (in Phase II) to find the best observing strategy that satisfies the science goals while following these guidelines as closely as possible.

6.2.2 Instrument Specific Limitations on Visits

For all science instruments, there are instrument-specific restrictions on the definition of a visit.

ACS and WFC3: Data Volume Constraints

If full frame ACS or WFC3 data are taken at the highest possible rate (~6 ACS/WFC or WFC3 images per nominal orbit, or ~12 images per CVZ orbit) for several consecutive orbits, it is possible to accumulate data faster than it can be transmitted to the ground. High data volume proposals will be reviewed and on some occasions, users may be requested to divide the proposal into different visits or consider using subarrays. Users can achieve higher frame rates by using subarrays, at the expense of having a smaller field of view; see the *ACS Instrument Handbook* or *WFC3 Instrument Handbook* for details.

FGS: Astrometry

For astrometric observations using FGS1R, each individual set (consisting of target object and reference objects) may be contained in one visit if there is no telescope motion made during the sequence.

Coronagraphy

Most STIS coronagraphic observations will likely be single visits that use the full orbit for science observations.

Proposals requesting two coronagraphic observations at different roll angles in the same orbit will have the following requirements:

- Each acquisition (ACQ) and its corresponding science exposures must be scheduled as a separate visit.
- Each visit must not exceed 22 minutes, including guide star acquisition, ACQ, exposure time, and overhead.
- No more than two ACQs within one orbit will be allowed. The effectiveness of the roll-within-an-orbit technique has been shown to depend heavily on the attitude of the telescope preceding the coronagraphic observation. Thus, using this technique does not guarantee cleaner PSF subtraction.

As an extra insurance policy, coronagraphic observers may want to consider adding an extra orbit for each new pointing. Thermal changes in the telescope are likely to be significantly smaller in the second and subsequent orbits on a target than in the first orbit.

Coronagraphic observations requiring particular telescope orientations (e.g., positioning a companion or disk between diffraction spikes) are time-critical and must be described in the 'Special Requirements' section of a Phase I proposal (see Section 9.3 of the Call for Proposals).

STScI will provide standard calibration reference files such as flat fields and darks for calibration purposes. Contemporary reference files in support of coronagraphic observations are not solicited or normally approved for GO programs, but coronagraphic observers who can justify the need for contemporary calibration observations must include the additional orbit request in the Phase I proposal. All calibration data (regardless of the program) are automatically made public.

STIS: CCD and MAMA Observations in the Same Visit

In order to preserve SAA-free orbits for MAMA observations, STIS programs that contain both CCD and MAMA science observations (excluding target acquisitions) must be split into separate CCD and MAMA visits. Exceptions to this rule may be allowed if one of the following three conditions is met:

- There is a well justified scientific need for interspersed MAMA and CCD observations.
- There is less than 30 minutes of science observing time (including overheads) using the CCD.
- The target is observed for only one orbit.

6.3 The Orbital Visibility Period

The *orbital visibility period* is the amount of unocculted time per orbit during which observations of a given target can be made. Table 6.1 gives the visibility period for fixed targets of given declination, for moving targets (assumed to be near the ecliptic plane), and for cases in which the special requirements **CVZ** (Section 2.2.1), **LOW SKY** (Section 8.16.12 of the Call for Proposals), and **SHADOW** (Section 8.16.12 of the Call for Proposals) are used.

The listed orbital visibility for the CVZ (96 minutes, i.e., the entire *HST* orbit) assumes that there are no SAA intersections in these orbits (see Section 2.2.2). This is the orbital visibility that should be used for planning CVZ observations, unless the proposer knows that he or she may have to observe in orbits that are SAA-impacted. In the latter case, the visibility time is approximately 70 minutes per orbit. During a CVZ window, only 5-6 true CVZ orbits (96 minutes) can be scheduled each day. Note that CVZ orbital visibility should *not* be requested if there are special background emission or timing requirements (see Section 2.2.1).

Also included in Table 6.1 are orbital visibilities suitable for use in Large Programs (see Section 3.2.2 of the Call for Proposals). Proposers submitting Large Programs should consult the Large Program Scheduling User Information Report which can be found on the *HST* Documents page (linked from the Cycle 25 Announcement webpage). This document contains a discussion of the issues surrounding Large Program scheduling.

Table 6.1: Orbital Visibility in Three-Gyro Mode.

Target	|Declination| (degrees)	Orbital Visibility (min)	LARGE visibility (min)	LOW visibility (min)	SHADOW visibility (min)
Moving	object near ecliptic plane	54	50	47	25
Fixed	0 – 30	54	50	47	25
Fixed	30 - 40	55	50	48	25
Fixed	40 - 50	57	50	48	25
Fixed	50 - 60	58	50	45	25
Fixed	60 – 70	59	50	45	25
Fixed	70 - 80	60	51	43	25
Fixed	80 - 90	61	52	42	25
Any	Any CVZ declination	96	96	incompatible	incompatible

Orbital Visibility Period for Pure Parallel Observations

For Pure Parallel observations (see Section 4.2.2 of the Call for Proposals), proposers may not know the prime target declinations. One of the following two options should be used for planning observations:

- Use the minimum allowed orbital visibility period for the target's selection criteria. For example, if the requirement calls for fields around M31 (at a declination of 50°), use 57 minutes.
- Map out the desired exposures (plus overheads) in an orbit for any legal orbital visibility period (54 to 61 minutes). If this method is selected, note that longer total exposure times typically have fewer scheduling opportunities.

6.4 Acquisitions Times and Instrument Overheads

The entire target orbital visibility for actual science exposures cannot be used because of the required times for guide star acquisition, target acquisition, and SI overheads. The following subsections discuss the amounts of time that should be budgeted for these items; they are conservative approximations suitable for use in a Phase I proposal and may differ slightly from the numbers in the instrument handbooks.

6.4.1 Guide Star Acquisition Times

A normal guide star acquisition, required in the first orbit of every visit, takes six minutes. At the start of subsequent orbits in a multi-orbit visit, the required guide star *reacquisition* takes four minutes. For CVZ observations, guide star reacquisitions are not required but, if an observation extends into SAA-impacted orbits (see Section 2.2.2), then guide star reacquisitions will be necessary for those orbits.

Table 6.2: Guide Star Acquisition Times

Type of acquisition	Acquisition time (minutes)	Use
Guide star acquisition	6	First orbit of every visit. Also applies to Snapshot observations.
Guide star reacquisition	4	All orbits of a multi-orbit visit, except the first orbit. May not be needed for CVZ observations (see text).

6.4.2 Target Acquisition Times

A target acquisition may be required after the guide star acquisition, depending on the science instrument (SI) used and pointing requirements. See Section 5.2 for a basic overview of target acquisitions. Consult the HST Instrument Handbooks to determine whether a target acquisition is required for particular types of observations, and which acquisition type is most appropriate. Table 6.4 can be used to determine the time budget for these activities.

Target acquisitions are commonly used for COS and STIS spectroscopy. A number of target acquisition options are provided for each instrument. In some cases, an additional set of peak-up observations can follow the initial instrument acquisition.

Most **normal imaging** observations with ACS, STIS, and WFC3 do not require target acquisitions (assuming that the coordinates delivered by the observer in Phase II have sufficient accuracy of 1" to 2"). Since the COS aperture has a small 2.5" diameter field of view, a target acquisition is recommended for COS imaging unless the coordinates supplied by the observer are accurate to 0.4" or better. For COS imaging, the same acquisition strategies are available as for spectroscopy.

Due to increased NUV detector background and mechanism position uncertainties, certain NUV central wavelength settings have proven to be unreliable in the ACQ/PEAKXD target acquisition step. The central wavelength settings below are settings that have been proven reliable. Spectroscopic NUV target acquisitions that use ACQ/PEAKXD must use one of the settings listed in Table 6.3. The most reliable settings for each grating are shown in bold, but any setting below may be used.

Table 6.3: List of NUV settings to use for ACQ/PEAKXD TAs.

G185M: 1786, **1913**, **1921**

G225M: 2637, **2657**, 2676, 2695

G285M: **2306**, 2357

G230L: **2635**, 2950, 3000

For **coronagraphic imaging** with STIS, a target acquisition is required to place the target behind the coronagraphic hole or feature. For STIS, the same ACQ and ACQ/PEAK strategies are available as for spectroscopy.

FGS observations use a so-called **"**spiral search**"** location sequence for target acquisitions. This is part of a science observation, and the time required for the acquisition is considered to be part of the overhead associated with the science observation (see Table 6.7).

Table 6.4: Target Acquisition Times

Scientific Instrument	Type of acquisition	Acquisition time (minutes)	Notes
COS	ACQ/IMAGE	3	Typical acquisition in NUV integrated light (recommended). Total time required is 2 min + (2 x exposure time.)
COS	ACQ/SEARCH ACQ/PEAKXD ACQ/PEAKD	14	Typical precision acquisition in dispersed light (for targets with either NUV or FUV). Total time required for full sequence is ~10 min. plus (15 x exposure time.)
STIS	ACQ	6	Used for STIS spectroscopy or coronagraphy. For faint targets (V > 20), add 4 times the acquisition exposure time determined by the Target Acquisition ETC.
STIS	ACQ/PEAK	6	Used for STIS spectroscopic observations in apertures <= 0.1" in size, or for any STIS spectroscopic observation that requires the highest possible absolute precision in the zeropoint of the wavelength scale.This type of target acquisition always follows an ACQ. For faint targets (V > 20), add 4 times the acquisition exposure time determined by the Target Acquisition ETC.

Generally, a target acquisition does not need to be repeated for separate orbits of a multi-orbit visit. However, for observers planning multi-orbit observations in 0.1" or smaller STIS slits, insertion of a target peak-up maneuver for every four orbits is recommended (see "FGS - Dual Guide Star Acquisitions").

A target acquisition, if necessary, should usually be inserted in each visit. However, programs with multiple visits to the same target within a six-week period (from start to finish) may be able to use the **Reuse Target Offset** function (see Section 5.2.2). If "reuse target offset" is appropriate for a program, then the observer should include the full target acquisition sequence only in the initial visit; subsequent visits will not need

a full target acquisition. However, a **Small Angle Maneuver** (SAM) may be required (see Section 6.4.4) for the offset maneuver, usually followed by the final peak-up stage used in the original acquisition. Please contact the STScI Help Desk (see Section 1.3.9) if this capability would benefit your program.

6.4.3 Instrument Overhead Times

There are a variety of instrument overheads associated with science exposures. Tables 6.5 to 6.10 summarizes, for each instrument, the amount of time needed to budget for overheads, depending on the observing strategy.

For several years, many observers have been using *dithering*, or small spatial displacements, to allow for better removal of detector defects and the reconstruction of sub-pixel resolution images. In general, *undithered* observations with the ACS CCD and WFC3 detectors will not be approved without strong justification that such observations are *required* for the scientific objectives (see Section 5.2.)

ACS

ACS exposure overheads are listed in Table 6.5. The overhead per exposure is shorter if the exposure is the same as the previous exposure (i.e., the exposures use the same aperture and spectral element, but not necessarily the same exposure times). If there is uncertainty about whether the shorter overhead time is appropriate, then use the longer overhead time (to avoid a possible orbit allocation shortfall).

Table 6.5: ACS Exposure Overheads

SI Mode	WFC Overhead time (minutes)	SBC Overhead time (minutes)	Notes
IMAGING/ SPECTROSCOPIC	4.0	1.7	A single exposure or the first exposure in a series of identical exposures.
IMAGING/ SPECTROSCOPIC	2.5	0.9	Subsequent exposures in an identical series of exposures.
IMAGING/ SPECTROSCOPIC	5.7	0	Buffer dump if exposure will exceed current buffer capacity and exposure is less than 337 seconds. (see the *ACS Instrument Handbook* for details)
SPECTROSCOPIC	N/A	N/A	Automatically executed (if AUTOIMAGE =YES) imaging exposure for prism spectroscopy (provides the image to co-locate the targets and their spectra; see the *ACS Instrument Handbook* for details).
SPECTROSCOPIC	7	N/A	Automatically executed (if AUTOIMAGE =YES) imaging exposure for grism spectroscopy (provides the image to co-locate the targets and their spectra; see the *ACS Instrument Handbook* for details).

Note that if AUTOIMAGE=NO is invoked and a different direct image is specified for the WFC spectroscopic calibration, and in all cases for the SBC calibration (for which there is no AUTOIMAGE due to the safety issue), these direct images must be included explicitly in the Observing Summary and the observing time (orbit) request of the Phase I proposal.

COS

An ACQ/SEARCH will require about seven minutes of overhead, while an ACQ/IMAGE requires three minutes. The combination of ACQ/PEAKXD and ACQ/PEAKD will also require seven minutes. The first science exposure in a visit requires five minutes, while subsequent identical exposures incur two minutes of overhead. An additional one minute is needed for each instrument change between exposures, except that incrementing the FP-POS at the same CENWAVE setting only requires three seconds if the ordering of the FP-POS positions is done correctly. COS exposure overhead are listed in Table 6.6

Table 6.6: COS Exposure Overheads

Acquisition or exposure	Overhead time (minutes)	Notes
Guide-star acquisition	6	First orbit of each visit
Guide-star reacquisition	4	Each subsequent orbit
ACQ/IMAGE	3	Typical imaging acquisition
ACQ/SEARCH	7	Imaging or dispersed, FUV or NUV
ACQ/PEAKXD+ACQ/PEAKD	7	Typical dispersed peakups, FUV or NUV
Science (imaging or dispersed)	5 2 1	First exposure in a series Each subsequent exposure Change of instrument configuration (except to increment FP-POS)

FGS

FGS overheads are listed in Tables 6.7 and 6.8. The total TRANS mode overhead consists of an acquisition overhead plus an overhead per scan. Hence, the total overhead depends on the number of scans obtained during a target orbital visibility period. Table 6.9 lists the recommended number of scans as a function of target magnitude. The recommended *exposure* time is 40 seconds per scan (excluding overheads).

Table 6.7: FGS Exposure Overheads

SI Mode	Overhead time (minutes)	Notes
POS	1	If target magnitude V < 14
POS	2	If target magnitude 14 < V < 15
POS	3	If target magnitude 15 < V < 16
POS	4	If target magnitude 16 < V < 16.5
POS	8	If target magnitude V > 16.5
TRANS	1	Target acquisition (independent of target magnitude)
TRANS	0.2	Overhead per scan (independent of target magnitude)

Table 6.8: FGS Miscellaneous Overheads

Type	Time [min.]
Instrument setup, per orbit	4
Instrument shutdown, per orbit	3

Table 6.9: Recommended number of FGS TRANS mode scans

Magnitude (V-band)	Number of scans
8 - 12	10
13 - 14	20
15	30
16	60

STIS

STIS overheads are listed in Table 6.10. The overhead per exposure is shorter if the exposure is the same as the previous exposure (“no change”); this means that the exposures use the same aperture, grating and central wavelength, but the exposure times need not be the same. If there is uncertainty over whether the shorter overhead time is appropriate, then use the longer overhead time.

Table 6.10: STIS Exposure Overheads

Configuration/Mode	Overhead time (minutes)	Notes
CCD IMAGING	5	Overhead per exposure.
CCD SPECTROSCOPIC	5	Overhead per exposure.
CCD SPECTROSCOPIC	2 (4)[1]	Overhead for a series of identical exposures extending more than ~40 min
CCD IMAGING/SPECTROSCOPIC	1	Overhead per exposure, if no change from the previous exposure.
MAMA IMAGING (FUV or NUV)	5	Overhead per exposure.
MAMA IMAGING (FUV or NUV)	1	Overhead per exposure, if no change from the previous exposure.
MAMA SPECTROSCOPIC (FUV or NUV)	8	Overhead per exposure.
MAMA SPECTROSCOPIC (FUV or NUV)	4 (6)[1]	Overhead for a series of identical exposures extending more than ~40 min
MAMA SPECTROSCOPIC (FUV or NUV)	1	Overhead per exposure, if no change from the previous exposure.

1. For medium resolution modes G140M, G230M, and G230MB, there are some wavelength-slit combinations that require longer AUTOWAVECAL exposure times. For each set of exposures totaling more than 2300 seconds at the same grating position for mode G230MB, an overhead of 4 minutes should be budgeted. For each set of exposures totaling more than 2300 seconds at the same grating position for modes G140M and G230M, an overhead of 6 minutes should be budgeted.

WFC3

WFC3 exposure overheads are listed in Table 6.11.

Table 6.11: WFC3 Instrument Overhead Times

Action	Overhead time (minutes)
Reconfiguration between UVIS and IR channels during a single orbit	1.0
Change quad filter (UVIS only)	1.0
UVIS ACCUM Mode	
Single exposure or first exposure in a set of identical exposures (e.g., the first sub-exposure of a CR-SPLIT set)	2.6
Subsequent exposures in set of identical exposures (e.g., subsequent exposures in a CR-SPLIT set), per exposure	2.1
Exposure with UVIS flash	0.1
Buffer dump if exposure is not last one in an orbit, or if next exposure is less than 339 seconds	5.8
IR MULTIACCUM Mode	
Each exposure	1.0
Buffer dump if 16-read exposure is not last one in an orbit, or if next exposure is less than 346 seconds	5.8

6.4.4 Telescope Repositioning Overhead Times

Small Angle Maneuvers (SAMs) are changes in telescope pointing of less than two arcminutes. Table 6.12 lists the overhead times for SAMs.

Table 6.12: Small Angle Maneuver Time

Step-size interval	SAM time (seconds)
0" < step-size < 1.25"	20
1.25" < step-size < 10"	30
10" < step-size < 28"	40
28" < step-size <60"	50
60" < step-size < 2'	65

A “Reuse Target Offset” visit (see Section 5.2.2 and Section 6.4.2) will require a SAM to be scheduled at the start of the first orbit. To allow for the offset adjustment, the SAM should be assumed to have a duration of 30 seconds.

Patterns described in Section 5.4 perform a series of SAMs. The timing and subsequent overheads depend on the size of the pattern. However, a simple estimate

for the overhead time associated with a pattern is obtained by multiplying the number of points minus 1 (one) times the overhead time for a single SAM (see Table 6.12) whose size matches the pattern spacing.

6.5 Constructing the Program

The final step is to efficiently pack all science exposures and overheads into the orbital visibility period of each orbit for all visits. For particularly complex programs, the APT Phase II orbit planner can be used for assessing the orbit layout. Please contact help@stsci.edu for assistance.

When placing observations into orbits and visits, note that exposures cannot be paused across orbits. For instance, if there is 20 minutes left in an orbit, only an exposure that takes 20 minutes or less (including overhead) can be placed in it. For a 30 minute exposure, all of it can be placed in the next orbit, or a 20 minute exposure can be placed at the end of the first orbit, and a second 10 minute exposure in the next orbit.

As an example, Table 6.13 shows the layout of a visit with two orbits of spectroscopic observations that require a target acquisition, but no SAMs and no special calibration observations. For simplicity, overheads are shown to occur after each exposure; in reality, some overheads occur before an exposure (e.g., a filter change) while others appear afterwards (e.g., readout time).

Table 6.13: Example Visit

Orbit 1	Guide star acquisition	Target acquisition	Overhead	Science exposure	Overhead	Earth occultation
Orbit 2	Guide star reacquisition	Science exposure	Overhead	Science exposure	Overhead	Earth occultation

More detailed examples for each of the SIs are given in Appendix A. Those examples are for common, simple uses of the instruments. For more complex examples and observing strategies, please consult the HST Instrument Handbooks (see Section 1.3).

Coordinated Parallel Observations

For a program with coordinated parallel observations (see Section 4.2.1 of the Call for Proposals), laying out the parallel observations into orbits and visits is fairly straightforward. The primary observations determine the orbit and visit structure, and the coordinated parallels should conform to the visit structure of the primary observations.

CHAPTER 7:

Data Processing and the *HST* Data Archive

In this chapter...

7.1 Routine Science Data Processing

Science data obtained with *HST* are sent to the TDRSS satellite system, from there to the TDRSS ground station at White Sands, New Mexico, then to the Sensor Data Processing Facility at Goddard Space Flight Center in Greenbelt, Maryland, and then finally to STScI.

At STScI, the production pipeline provides standard processing for data editing, calibration, and product generation. These functions, performed automatically, include the following:

- Reformatting and editing of data from the spacecraft packet format to images or spectra.
- Performing standard calibrations (flat fields, wavelength calibrations, background subtraction, etc.) with best available calibration files.
- Producing standard data output products (FITS format files of raw and calibrated images, OMS [jitter and performance flags] files).

Standard calibrations performed on *HST* data, and the resulting output data products, are described in detail in the HST Data Handbook.

In 2015, major upgrades to the Science Data Processing Pipelines (DP) and Data Distribution System (DADS) were installed. Archive users will now find HST data stored on disks for immediate download. Data will be reprocessed, as needed, when updated calibration reference files or improved calibration algorithms are received to ensure the freshest data are available for users. Data from all non-active instruments (HSP, GHRS, FOC, FOS, WF/PC, WFPC-2 and NICMOS) continue to be available for direct download. In the event a dataset is requested when those data are queued for reprocessing, the user will experience a delay as those data are processed through the system at a higher priority before being delivered.

7.1.1 Space Telescope Science Data Analysis System (STSDAS)

The Space Telescope Science Data Analysis System (**STSDAS**), and its accompanying package, **TABLES**, provides access to applications for the analysis of HST data as well as various utilities for manipulating and plotting data. The **TABLES** package facilitates the manipulation of FITS table data. **STSDAS** and **TABLES** were originally layered onto the Image Reduction and Analysis Facility (**IRAF**) software from the National Optical Astronomy Observatories (NOAO). Both packages run from within **IRAF** and are supported on a variety of platforms, although not all of the platforms that IRAF supports.

All the existing calibration pipeline programs used by STScI to process all HST data can found in the **HSTCAL** package, a package which allows users to compile and run the calibration software originally written in C without using or running **IRAF**. The latest versions of all the active instruments' calibration software no longer relies on **IRAF** and has been installed as the **HSTCAL** package for Archive and pipeline operations. HST observers can use the programs in **HSTCAL** to recalibrate their data, to examine intermediate calibration steps, and to re-run the pipeline using different calibration switch settings and reference data as appropriate.

These **HSTCAL** software versions replace the calibration software available under **STSDAS**; specifically, **CALACS** for ACS, **CALWF3** for WFC3, and **CALSTIS** for STIS.

Much of the newer calibration and analysis software is written in Python, including **CALCOS** for COS data. It does not require **IRAF**, and is available as part of the STScI Python library included and installed as part of Ureka releases.

PyRAF is an alternate Python-based command-line environment that enables users to run **IRAF** tasks and allows the new Python-based software to be used, along with **IRAF** tasks, with **IRAF** command-line syntax. Ureka includes **astropy**, a set of packages that provides Python programs the ability to read and write FITS files and read and manipulate the WCS information in image headers. The new Python environment allows users to manipulate and display data in a way not possible with

IRAF that is more akin to how data can be manipulated and displayed by ***IDL*** (Interactive Data Language). The STScI Python environment described above is contained within the **stsci_python** package. Detailed information on **STSDAS**, **TABLES**, PyRAF, Ureka, and other Python-based software, including the actual software, is available from the STScI Software webpage. Information about **IRAF** is available from the IRAF webpage.

7.2 The *HST* Data Archive

All science and calibration data are placed in the HST Data Archive. Science data become immediately available (after pipeline processing) to a program's Principal Investigator (PI), as well as those designated by the PI as long as they are authorized to retrieve the data. These data may be retrieved after the PI has registered for an STScI single sign-on (SSO) account and are normally proprietary for a period of six months from the date of observation (see Section 5.1 of the Call for Proposals for information on data rights).

On average, science data from HST flow through the production pipeline and into the Archive within one day after observation on the telescope. Some data may take as long as three to five days. Observers are notified by e-mail when the first datasets reach the Archive. They are also provided with Web tools to track a visit's completeness and to retrieve the data generated by the pipeline.

The time required for retrieving data from the Archive depends on whether the data are available for direct download or need to be reprocessed, the speed of the user's connection, the size of the requested dataset, and the load on the Archive. As of October 1, 2016, the HST Data Archive contains over 126 TB of data. During the first quarter of 2017, all of the HST data, including proprietary data, should be online and available for direct download through the Data Discovery Portal. To retrieve proprietary data users must have a MyST account and be authorized to do so.

If there are strict scientific requirements for data receipt within days after execution, such as to provide pointing corrections for tightly scheduled visits, there are resource-intensive methods to expedite delivery of data. Such requirements must be stated in the proposal so that the resource needs can be determined and reviewed (see Section 9.3 of the Call for Proposals).

7.2.1 Web Access to the *HST* Data Archive

Most of the data in the HST Data Archive are public and may be retrieved by any user.

The Archive may be accessed through a number of web-based interfaces. The dedicated HST search page, also available under the "Mission Search" menu tab at the MAST webpage, allows qualified searches for HST data, and download of those data and their reference files. The MAST Portal provides a number of capabilities to search for, inspect, and download data. Its interface includes integrated access to the Digitized Sky Survey (DSS) and enables users to access a coordinate resolver to look up the coordinates of an object by name. In both interfaces it is possible to request specific data products instead of the entire complement of files. Requesters of proprietary data will be required to log in to their MyST Single Sign-On (SSO) System account. Starview only allows searches of instrument-specific databases and requires users to sign in using their SSO account. All of the MAST search interfaces provide previews of most publicly available images and spectra.

STScI maintains an "Archive Helpdesk" for all archive-related questions, problems, or comments. The Archive Helpdesk can be reached by e-mail at archive@stsci.edu or by phone at 410-338-4547.

7.3 Hubble Legacy Archive (HLA)

The Hubble Legacy Archive (HLA) is a project designed to enhance science from the Hubble Space Telescope by augmenting the *HST* Data Archive and by providing advanced browsing capabilities. It is a joint project of the Space Telescope Science Institute, the Canadian Astronomy Data Centre (CADC), and the European Space Astronomy Centre (ESAC). The primary enhancements are:

- Advanced data products with several *HST* instruments, produced for public data.
- Data products that are immediately available online for viewing, searching and downloading.
- A footprint service that makes it easier to browse and download images.
- Availability of combined images, prototype mosaics, and spectral data.
- For many images, the absolute astrometry has been improved from one to two arcsec to ~0.3 arcsec.
- Source lists are available for ACS, WFPC2, and WFC3 observations.
- NICMOS and ACS grism extractions have been produced by European Coordinating Facility (ST-ECF).
- An interface is provided for many user-provided High Level Science Products.

At the time of this writing (November 2016), the HLA has completed its ninth major Data Release, including enhanced data products for almost all public science data for WFC3, ACS, WFPC2 (produced by CADC) and NICMOS. Also available are source lists for ACS, WFPC2, and WFC3. Some STIS spectra are also available as high level science products, and can be searched, viewed, and retrieved through the same interface as enhanced image data. Multi-visit ACS mosaics have been produced for 67 pointings. The footprint service shows the outline of data from all instruments, including data that are still proprietary, and an interface to the main HST Archive is provided to access proprietary data (for PIs and their designated collaborators) and recent data for which enhanced HLA products are not yet available.

Some of the more general goals of the HLA are to make HST data VO-compatible (Virtual Observatory), to move toward a sky atlas user view rather than a collection of datasets, and to develop an "all-HST-sky" source list. The Hubble Source Catalog (HSC), described in more detail in Section 7.4, represents a major milestone toward the attainment of these goals for the HLA.

The HLA can be accessed at: http://hla.stsci.edu.

7.4 Hubble Source Catalogs (HSC)

As described in Section 7.3, the HLA produces source lists for tens of thousands of HST images. The Hubble Source Catalog (HSC) combines these single, visit-based WFC3, ACS, and WFPC2 source lists into a single Master Catalog, hence providing entry into the field of database astronomy. Searches that would require months or years to perform in the past can in many cases be done in seconds with the HSC. This resource may be used to support a wide range of new archival proposals, a few potential examples of which are listed below.

Version 2 of the Hubble Source Catalog was released in the fall of 2016. The primary improvements from version 1 were the addition of four years of ACS data and the cross matching of the HSC with spectral observations from COS, FOS and GHRS. A journal-level publication describing the HSC, quality of the data, and potential for doing science is available at Whitmore et al. (2016). A FAQ describing most aspects of the HSC is available. The matching algorithms used by the HSC are described in Budavari & Lubow, 2012.

The HSC can be accessed in a variety of ways. For most cases, the best method will be the MAST Discovery Portal (DP). This Virtual Observatory (VO)-based tool provides easy yet powerful access for searches involving 50,000 or less. It provides footprints, object selection filtering, and interactive displays. For larger queries, a powerful CASJobs (CAS = Catalog Archive Server) capability is available[1]. This resource is

based on the Sloan Digital Sky Survey (SDSS) tool[2], providing similar support into the world of database astronomy.

Below is a list of some of the types of projects that might make particularly good use of this new resource.

- Variable stars, galaxies, calibrations, etc., identified using HST's ~25 year baseline. Note: a project to construct a Hubble Variable Catalog is underway, headed by the National Observatory of Athens.
- Astrometric properties: proper motions, cluster kinematics, KBOs, etc.
- Extremely large data sets: e.g., creating CMDs based on the ~ 4000 HST observations of the LMC.
- Cross-matching with other catalogs: SDSS, 2MASS, spectral catalogs, etc.
- Object properties: star clusters and associations, colors, elongations, etc.
- Photo-Zs.
- Compilation of spectroscopic properties based on COS, FOS, and GHRS observations, cross-matched with their HSC counterparts.

1. A third method of access is via the HSC homepage. This provides the most flexibility for very detailed queries.

2. A word of *caution* is in order, however. Unlike SDSS, with a uniform set of filters and all-sky coverage over a substantial part of the sphere, the Hubble database consists of tiny pieces of sky using three different cameras and hundreds of filters. Potential users should pay special attention to the Five Things You Should Know About the HSC webpage. Detailed use cases are available to guide users in common ways to make use of the HSC and to avoid common pitfalls.

APPENDIX A:

Orbit Calculation Examples

In this appendix...

A.1 ACS Example

The ACS WFC channel is used to observe a target at declination +35°. The requested exposures are listed in Table A.1.

- According to Table 6.1, there are 55 minutes of orbital visibility per orbit.
- Overheads for the observations, documented in Chapter 6, are compiled in Table A.2.

Therefore, a preliminary observing strategy can be created by the user to fit the observations in two orbits, as shown in Table A.3.

Table A.1: ACS Example: Planned Exposures

Config	Mode	Spectral Element	Number of exposures	Time per exposure (minutes)	Notes
ACS/WFC	IMAGING	F606W	4	8.75	Pattern (see Section 5.4) with an offset of 25" between positions
ACS/WFC	IMAGING	F814W	4	9.0	Same as above.

Table A.2: ACS Example: Incurred Overheads

Overhead	Overhead time (minutes)	Notes	see Table
Guide star acquisition	6	First orbit in new visit	6.2
Guide star reacquisition	5	Per orbit after first orbit	6.2
WFC exposure (first)	4	First exposure in a series of identical exposures	6.5
WFC exposure (not first)	2.5	Per exposure after the first exposure in a series	6.5
SAM of 25"	0.67	Small Angle Maneuver between positions in the pattern	6.13

Table A.3: ACS Example: Orbit Planning

Activity	Duration (minutes)	Elapsed Time (minutes)
Orbit 1		
Guide star acquisition	6	6
WFC/F606W Exp Time	4x8.75	41
WFC/F606W Overhead	4+(3x2.5)+(3x0.67)	54.5
Unused time	0.5	55
Orbit 2		
Guide star reacquisition	5	5
WFC/F814W Exp Time	4x9.0	41
WFC/F814W Overhead	4+(3x2.5)+(3x0.67)	54.5
Unused time	0.5	55

A.2 COS Examples

This section illustrates two examples of COS Phase I observations. Additional details are available in the *COS Instrument Handbook*.

A.2.1 Example 1: COS NUV Imaging and Spectroscopy in One Orbit

The COS NUV channel is used to observe an object at declination -10^{o}. First, an image is taken, followed by obtaining a TIME-TAG spectrum with two exposures using different gratings. The specific observations, as requested by the user, are summarized in Table A.4.

- Based on information in Table 6.1, there are 54 minutes of orbital visibility per orbit.
- Overheads for the observations, documented in Chapter 6, are compiled in Table A.5.

Therefore, a preliminary observing strategy can be created by the user to fit the observations in one orbit, as shown in Table A.6. In this example, we assume that the coordinates of the object are known to an accuracy of 0.4 arcsec or better. See the *COS Instrument Handbook* for details.

Table A.4: COS Example 1: Planned Exposures

Config	Mode	Spectral element	Number of exposures	Time per exposure (seconds)	Notes
COS/NUV	ACQ/IMAGE	MIRRORA	1	20	target acquisition
COS/NUV	TIME-TAG	G185M	1	1200	central wavelength 1850 Å
COS/NUV	TIME-TAG	G225M	1	600	central wavelength 2250 Å

Table A.5: COS Example 1: Incurred Overheads

Overhead	Overhead time (minutes)	Notes	see Table
Guide star acquisition	6	First orbit in new visit	6.2
ACQ/IMAGE	3	Target acquisition	6.4
NUV spectroscopy	5	Single spectroscopic exposure	6.6

Table A.6: COS Example 1: Orbit Planning

Activity	Duration (minutes)	Elapsed time (minutes)
Orbit 1		
Guide star acquisition	6	6
ACQ/IMAGE	3	9
G185M Overhead	5	13
G185M Exp time	20	34
G225M Overhead	5	39
G225M Exp time	10	49
Unused	2	54

A.2.2 Example 2: COS NUV Imaging and FUV Spectroscopy in Two Orbits

The COS NUV channel is used to acquire the same object as in Example 1, in imaging mode, then uses the FUV channel to obtain a TIME-TAG spectrum with two exposures using the same grating and central wavelength. The planned exposures are summarized in Table A.7.

- Based on information in Table 6.1, there are 54 minutes of orbital visibility time per orbit.
- Overheads for the observations, documented in Chapter 6, are compiled in Table A.8.

Therefore, a preliminary observing strategy can be created by the user to fit the observations in two orbits, as shown in Table A.9. In this example, we assume that the coordinates of the object are known to an accuracy of 0.4 arcsec or better. See the *COS Instrument Handbook* for details.

Table A.7: COS Example 2: Planned Exposures

Config	Mode	Spectral element	Number of exposures	Time per exposures (seconds)	Notes
COS/NUV	ACQ/IMAGE	MIRRORA	1	30	Target acquisition
COS/FUV	TIME-TAG	G160M	1	2100	Central wavelength 1600 Å
COS/FUV	TIME-TAG	G160M	1	2700	Central wavelength 1600 Å

Table A.8: COS Example 2: Incurred Overheads

Overhead	Overhead time (minutes)	Notes	see Table
Guide star acquisition	6	First orbit in new visit	6.2
Guide star reacquisition	4	Per orbit after first orbit	6.2
ACQ/IMAGE	3	Target acquisition	6.4
FUV spectroscopy	5	First spectroscopic exposure in a series of identical exposures	6.6
FUV spectroscopy	2	Subsequent spectroscopic exposure in a series of identical exposures	6.6

Table A.9: COS Example 2: Orbit Planning

Activity	Duration (minutes)	Elapsed time (minutes)
Orbit 1		
Guide star acquisition	6	6
ACQ/IMAGE	3	9
G160M Overhead	5	14
G160M Exp time	35	49
Unused	5	54
Orbit 2		
Guide star reacquisition	4	4
G160M Overhead	2	6
G160M Exp time	45	51
Unused	3	54

A.3 FGS Example

The FGS is used to observe a binary star named Binary01, as well as five reference stars (ref1, ref2, ref3, ref4, ref5). All stars are in the same FGS field of view, and can therefore be observed in one visit (see Section 6.2.2). Stars ref4 and ref5 have magnitude V = 14.6, and all the other targets have 13.0 < V < 14.0. To enable the removal of drift and jitter in the post observation analysis of the data, the Binary01 is observed in POS mode several times (twice in this example) and the reference stars are each observed twice. The desired exposures are listed in Table A.10,

- The targets have a declination of +42°, which gives 57 minutes of orbital visibility per orbit (see Table 6.1).
- The associated overheads are listed in Table A.11.

Therefore, a preliminary observing strategy can be created by the user to fit the observations in one orbit, as shown in Table A.12.

Table A.10: FGS Example: Planned Exposures

Config	Mode	Spectral element	Number of exposures	Time per exposure (minutes)	Notes
FGS	POS	F583W	8	0.6	Two exposures of target Binary01, and two exposures for each of the targets ref1, ref2, and ref3
FGS	POS	F583W	4	1.1	Two exposures for each of the targets ref4 and ref5
FGS	TRANS	F583W	1	13.4	20 scans of 40 sec each (see Table 6.7) for Binary01

Table A.11: FGS Example: Incurred Overheads

Overhead	Overhead time (minutes)	Notes	see Table
Guide star acquisition	6	First orbit in new visit	6.2
POS	1	Per exposure, V < 14	6.8
POS	2	Per exposure, 14 < V < 15	6.8
TRANS	1	Per target	6.8
TRANS	0.2	Per scan	6.8
Instrument Setup	4	Once every orbit	6.9
Instrument Shutdown	3	Once every orbit	6.9

Table A.12: FGS Example: Orbit Planning

Activity	Duration (minutes)	Elapsed time (minutes)
Orbit 1		
Guide star acquisition	6	6
Instrument Setup	4	10
Binary01/POS mode Exp Time	0.6	10.6
Binary01/POS mode Overhead	1	11.6
ref1/POS mode Exp Time	0.6	12.2
ref1/POS mode Overhead	1	13.2
ref2/POS mode Exp Time	0.6	13.8
ref2/POS mode Overhead	1	14.8
ref3/POS mode Exp Time	0.6	15.4
ref3/POS mode Overhead	1	16.4
ref4/POS mode Exp Time	1.1	17.5
ref4/POS mode Overhead	2	19.5
ref5/POS mode Exp Time	1.1	20.6
ref5/POS mode Overhead	2	22.6
Binary01/POS mode Exp Time	0.6	23.2
Binary01/POS mode Overhead	1	24.2
ref1/POS mode Exp Time	0.6	24.8
ref1/POS mode Overhead	1	25.8
ref2/POS mode Exp Time	0.6	26.4
ref2/POS mode Overhead	1	27.4
ref3/POS mode Exp Time	0.6	28
ref3/POS mode Overhead	1	29
ref4/POS mode Exp Time	1.1	30.1
ref4/POS mode Overhead	2	32.1
ref5/POS mode Exp Time	1.1	33.2
ref5/POS mode Overhead	2	35.2
Binary01/TRANS mode Exp Time	13.4	48.6
Binary01/TRANS mode Overhead	1+(20x0.2)	53.6
Instrument Shutdown	3	56.6
Unused	0.4	57.0

A.4 STIS Example

STIS is used to observe a target at a declination of +15° degrees according to an observing strategy outlined in Table A.13.

- For a target at declination of +15°, there are 54 minutes of orbital visibility per orbit (see Table 6.1).
- The associated overheads for those types of observations are listed in Table A.14.

Therefore, a preliminary observing strategy can be created by the user to fit the observations in two orbits, as shown in Table A.15.

Table A.13: STIS Example: Planned Exposures

Config	Mode	Spectral element	Number of exposures	Time per exposures (minutes)	Notes
STIS/CCD	ACQ			0.1	Target acquisition
STIS/CCD	ACQ/PEAK			1	Peakup acquisition (necessary because of use of 0.1" wide slit for subsequent spectra)
STIS/CCD	IMAGING	F28X50OII	2	2	
STIS/NUV	IMAGING	F25QTZ	1	21	
STIS/NUV	SPECTROSCOPIC	G230L	1	13	with 52X0.1 slit
STIS/FUV	SPECTROSCOPIC	G140L	1	20	with 52X0.1 slit

Table A.14: STIS Example: Incurred Overheads[1]

Overhead	Overhead time (minutes)	Notes	see Table
Guide star acquisition	6	First orbit in new visit	6.2
Guide star reacquisition	4	Per orbit after first orbit	6.2
ACQ	6	Target acquisition	6.4
ACQ/PEAK	6	Peakup target acquisition	6.4
CCD imaging (first)	5	First exposure in a series of identical exposures	6.10
CCD imaging (not first)	1	Per exposure after the first exposure in a series	6.10
MAMA imaging	5	First exposure	6.10
MAMA spectroscopy	8	Only 1 minute if there is no change from first exposure. Add 4 minutes (6 minutes for modes G140M and G230M) for each exposure time interval that exceeds 2300 seconds at the same grating position.	6.10

Table A.15: STIS Example: Orbit Planning

Activity	Duration (minutes)	Elapsed time (minutes)
Orbit 1		
Guide star acquisition	6	6
ACQ	6	12
ACQ/PEAK	6	18
F28X50OII Exp Time	2x2	22
F28X50OII Overhead	5+1	28
F25QTZ Exp Time	21	49
F25QTZ Overhead	5	54
Unused	0	54
Orbit 2		
Guide star reacquisition	4	4
G230L Exp Time	13	17
G230L Overhead	8	25
G140L Exp Time	20	45
G140L Overhead	8	53
Unused	1	54

A.5 WFC3 Examples

A.5.1 Example 1: IR, 1 orbit, 2 filters

The WFC3 IR channel is used to obtain images of a target in filters F110W and F160W. Assume that the ETC has shown that exposure times of 10 minutes for F110W and 20 minutes for F160W are adequate for the science goals. These exposure times can be achieved with the up-the-ramp MULTIACCUM sequences SPARS50 (11.7 min) and SPARS100 (23.4 min), respectively. Also assume an orbital visibility[2] of 54 minutes. A summary of the orbit calculations is shown in Table A.6.

1. These overheads are for budgeting purposes. The actual overhead incurred depends upon the particular spectral element selected since the overhead to move the grating is position-dependent and the time for an auto-wavecal is mode-dependent. Additional efficiencies, such as executing auto-wavecals during guide star reacquisitions or occultation, that may be realized from fine-tuning of the actual exposures (but cannot be assumed a priori), are not included.

2. Information about orbital visibility as a function of declination is available in Chapter 6.

Table A.16: Orbit Calculation for WFC3 Example 1

Action	Time (minutes)	Explanation
Guide-star acquisition	6.0	Needed at start of observation of new target
IR overheads for 2 exposures	2 × 1.0 = 2.0	Includes filter changes, camera set-ups, and readouts
Science exposure in F110W	11.7	
Science exposure in F160W	23.4	
Total time used	43.1	

The total time used in the orbit shows that the target can be imaged in the selected filters within one orbit. Furthermore, the first exposure can be dumped from the buffer during the second exposure. The approximately nine minutes of unused time could be used for an additional exposure, during which the second exposure would be dumped.

A.5.2 Example 2: UVIS, Dithering, 2 Orbits, 1 Filter

This example illustrates the orbit calculation for a UVIS observation with a WFC3 UVIS box dithering pattern, which implements imaging at four pointings. The goal of the observation is to obtain a dithered image of a field such that it bridges the ~1 arcsec inter-chip gap between the UVIS CCDs when the images are combined.

For the purposes of this example, the following conditions are adopted: (1) the exposure time necessary to reach the desired signal-to-noise ratio is 80 minutes. (2) The orbital visibility for each orbit is 58 minutes. (3) Assume that cosmic ray removal will be done using the **drizzlepac** package; therefore the exposure will not be broken into sub-exposures. (4) One 20 minute exposure is obtained at each pointing in a four-point dither, taken over two orbits.

The orbit calculation for this visit is shown in Table A.17. Note that for a two arcsec offset maneuver, the three dither offsets will take 0.5 minutes each.

Table A.17: Orbit Calculation for WFC3 Example 2

Action	Time (minutes)	Explanation
Orbit 1		
Guide-star acquisition	6.0	Needed at start of observation of new target
UVIS overhead for first exposure	2.6	Includes filter change, camera set-up, and readout
UVIS overhead for second exposure	2.1	Includes readout
Spacecraft maneuver	0.5	To offset from first to second dither pointing
Two science exposures	$2 \times 20 = 40.0$	Exposures at the first two pointings in the dither pattern
Total time used in orbit 1	51.2	
Orbit 2		
Guide star reacquisition	5.0	Needed at start of new orbit to observe same target
UVIS overheads for 3rd and 4th exposures	$2 \times 2.1 = 4.2$	Includes readouts
Spacecraft maneuvers	$2 \times 0.5 = 1.0$	To offset to the 3rd and 4th dither pointings
Two science exposures	$2 \times 20 = 40.0$	Exposures at the final two pointings in the dither pattern
Total time used in orbit 2	50.2	

No overhead is incurred to dump the exposures because they are all longer than 339 seconds. Thus the desired exposures can be accomplished within the two orbits, and there are about seven to eight minutes of unused orbital visibility per orbit that could be used to increase the exposure times.

APPENDIX B:

HST Mission

In this appendix...

B.1 Servicing Missions and Instrument Complements

The Hubble Space Telescope (*HST*) is a cooperative project of the National Aeronautics and Space Administration (NASA) and the European Space Agency (ESA) to operate a long-lived space-based observatory for the benefit of the international astronomical community. *HST* was first conceptualized in the 1940s, designed and built in the 1970s and 80s. In April 1990, the Space Shuttle Discovery deployed *HST* in low Earth orbit (~600 kilometers). The initial complement of Scientific Instruments (SIs) was:

- The Fine Guidance Sensors (FGSs).
- The Faint Object Camera (FOC).
- The Faint Object Spectrograph (FOS).
- The Goddard High Resolution Spectrograph (GHRS).
- The High Speed Photometer (HSP).
- The Wide Field and Planetary Camera (WF/PC).

Soon after deployment, it was discovered that the primary mirror suffers from spherical aberration, which limited the quality of *HST* data obtained in the first few years of operation.

B.1.1 Servicing Mission 1 (SM1)

During servicing mission 1 (SM1) in December 1993, Space Shuttle astronauts successfully refurbished *HST*. They replaced the HSP with COSTAR, a corrective optics package. COSTAR's reflecting optics were deployed into the optical paths of the FOC, FOS, and GHRS, which removed the effects of the primary mirror's spherical aberration. The performance of the FGSs was unaffected by COSTAR. The WF/PC was replaced by a new instrument: the Wide Field and Planetary Camera 2 (WFPC2). It contained its own internal optics to correct the spherical aberration of the primary mirror.

The astronauts also installed new solar arrays. This resolved the problem of thermal vibrations, which affected the old arrays during day/night transitions and, in turn, degraded the telescope's pointing performance.

B.1.2 Servicing Mission 2 (SM2)

During servicing mission 2 (SM2) in February 1997, astronauts replaced the FOS and the GHRS with two new instruments:

- The Near Infrared Camera and Multi-Object Spectrometer (NICMOS).
- The Space Telescope Imaging Spectrograph (STIS).

FGS1 was also replaced with an enhanced FGS, called FGS1R. It has an adjustable fold-flat mirror which is commandable from the ground. This enables realignment in the FGS optical path to lessen the effects of the primary mirror's spherical aberration. As a result, the astrometric performance of FGS1R significantly exceeded that of the original FGS, resulting in FGS1R being designated the primary science FGS.

B.1.3 Loss and Recovery of NICMOS

NICMOS was unavailable for science operations between January 1999 and June 2002 (mid-Cycle 8 through Cycle 10); just after the SM2 launch, a thermal short in the NICMOS dewar caused the early exhaustion of its solid nitrogen cryogen, reducing the lifetime of the instrument to only about 2 years–the cryogen was depleted by January 1999.

During Servicing Mission 3B (SM3B) in March 2002, the installation of the NICMOS Cooling System (NCS), a mechanical cryo cooler, reactivated NICMOS operation, and restored infrared capability to HST. The temperature of the detectors using the mechanical cryo cooler were slightly warmer than before, so many NICMOS parameters were different during this second epoch of operation. Most notably the detector quantum efficiency (DQE) increased by ~30% to 50%.

NICMOS continued to operate until September 2008, when the NICMOS Cooling System (NCS) failed to cool down the instrument, following a warm-up due to a planned safemode. The instrument was not successfully restarted after Servicing Mission 4.

B.1.4 Servicing Missions 3A (SM3A) and 3B (SM3B)

HST has six rate-sensing gyroscopes on board. In the years after SM2, gyroscopes failed at a higher than expected rate, ultimately leading to a halt of *HST* observing in November 1999. In anticipation of this event, servicing mission SM3, which had been in planning for several years, was split into two separate missions: SM3A and SM3B.

SM3A

In December 1999, Space Shuttle astronauts lifted off for servicing mission SM3A. Six new gyroscopes were successfully installed, which allowed *HST* to resume normal operations.

Along with the gyro replacements, the *HST* Project used this "unplanned" mission to make other planned upgrades and refurbishments:

1. Voltage/temperature Improvement Kits (VIKs) were installed to help regulate battery recharge voltages and temperatures.
2. The original DF224 spacecraft computer was replaced by a 486 upgrade, which provides a significant improvement in onboard computing power.
3. FGS2 was replaced by a refurbished fine guidance sensor, FGS2R, to enhance the performance of the pointing and control system (see Appendix B.1.2). However, FGS1R remains the best choice for science observations due to its superior angular resolution.
4. The second tape recorder was replaced by a second Solid State Recorder (SSR), and a new transmitter was installed to replace one that had failed.

All of the upgrades underwent successful in-orbit verification and calibration, restoring the observatory's functionality as planned.

SM3B

Servicing Mission 3B was carried out during the first ten days of March 2002. During this mission, astronauts replaced the FOC with a new instrument, the Advanced Camera for Surveys (ACS).

Astronauts also installed the NICMOS Cooling System (NCS) to allow further use of NICMOS, which had exhausted its cryogen in January 1999. Installation of new solar arrays, electrical upgrades to the spacecraft's power control unit, along with various other engineering upgrades including an orbit reboost, were performed. After the servicing mission, the ACS and NICMOS instruments, as well as WFPC2, remained fully commissioned for science. STIS also operated nominally until it failed in August of 2004, but was restored to full functionality during SM4.

B.1.5 Loss of STIS

The Space Telescope Imaging Spectrograph (STIS) Side-2 electronics failed in August of 2004, during Cycle 13. The instrument was maintained in safe mode until its recovery during SM4.

B.1.6 Loss of ACS Wide Field Camera and High Resolution Camera

During Cycle 15, ACS WFC and HRC became unavailable for observations due to a failure in the electronics. The two cameras remained powered off until SM4.

B.1.7 SM4

Servicing Mission 4 (SM4) started with the Atlantis launch on May 11, 2009 and was completed, upon return of the Shuttle, on May 24, 2009. Space Shuttle astronauts installed two new instruments, the Wide Field Camera 3 (WFC3) and the Cosmic Origins Spectrograph (COS), together with a new set of gyros and other flight hardware. WFC3 replaced the Wide Field Planetary Camera 2 (WFPC2) as the on-axis instrument; COS replaced COSTAR.

The Space Telescope Imaging Spectrograph (STIS), that had suffered a serious electronics failure in August 2004, was fixed. The ACS repair successfully recovered the ACS/WFC that had ceased to be operational with the ACS/HRC in January 2007 due to an electronics failure. The Advanced Camera for Surveys Wide Field Camera (ACS/WFC) and the Solar Blind Channel (ACS/SBC) are now operating nominally. The High Resolution Channel (ACS/HRC) could not be recovered during SM4. The Near Infrared Camera and Multi-Object Spectrometer (NICMOS) is still on board *HST* but is no longer in service.

HST is expected to continue to operate in three-gyro mode for the foreseeable future.

APPENDIX C:

Legacy Instruments

In this appendix...

C.1 Faint Object Camera (FOC)

The FOC was designed to provide high resolution images of small fields. It consisted of two independent optical relays that magnified the input beam by a factor of four (f/96) and two (f/48). A variety of filters, prisms (for slitless spectroscopy), and polarizers could be placed in the optical beam. The f/48 relay also had a longslit spectrograph. The FOC photocathodes limited the wavelength range from 1200 Å to 6000 Å.

When corrected by COSTAR, the field of view (FOV) and pixel size of the f/96 camera were 7" x 7" (512 x 512 format) and 0.014" x 0.014", respectively; a field of 14" x 14" could be used with the 512 x 1024 pixel format and a rectangular pixel size of 0.028" x 0.014". Without COSTAR in the beam, the corresponding parameters for the f/96 camera were: 11" x 11" FOV in the 512 x 512 format with pixel size 0.0223" x 0.0223", and full-format field of 22" x 22" with 0.0446" x 0.0223" pixels. The corresponding values for the (little used) f/48 camera were twice those of the f/96 camera.

The f/96 camera was the primary FOC imaging workhorse. High voltage instabilities limited the use of the f/48 relay to mainly long-slit spectroscopy after the installation of COSTAR.

Most of the FOC data in the Archive are unique because the spatial resolution of the FOC is greater than that of any other *HST* instrument. Also, the UV sensitivity was significantly higher than WFPC2, but less than STIS, although a larger variety of filters was available. Finally, polarizers in the f/96 relay had very low instrumental polarization and excellent polarizing efficiencies.

A major reprocessing of the entire FOC science archive (science and non-science data) has been completed by ST-ECF, CADC, and STScI. This effort substantially improves the data quality and homogeneity. For more information about the reprocessed data, see ISR FOC-99. The reprocessed data have been incorporated into the *HST* Archive and are available through MAST.

C.2 Faint Object Spectrograph (FOS)

The FOS performed low and moderate resolution spectroscopy (R ~250 and 1300) in the wavelength range from 1150 Å to 8500 Å. A variety of apertures of different sizes and shapes were available to optimize throughput and spectral or spatial resolution. Ultraviolet linear and circular spectropolarimetric capabilities were also available.

The low resolution mode had two gratings and a prism, and the R = 1300 mode had six gratings to cover the entire spectral range. The photon counting detectors consisted of two 512-element Digicons, one which operated from 1150 Å to 5500 Å (FOS/BLUE), and the other from 1620 Å to 8500 Å (FOS/RED).

Most FOS data were acquired in accumulation and rapid-readout modes; periodic and image modes were used infrequently. Time resolutions as short as 30 msec were feasible. The electron image was magnetically stepped through a programmed pattern during the observations which provided for oversampling, compensation for sensitivity variations along the Digicon array, sky measures, and/or measurement of orthogonally polarized spectra. Normally, data were read out in intervals that were short compared to the exposure time.

The FOS received about 20% to 25% of the total *HST* observing time over Cycles 1 to 6, studying a large and diverse range of science topics. Due to the polarimetric and large dynamic range capabilities, a substantial fraction of these data is and will remain unique.

A major reprocessing of the entire FOS archive has been completed at the Space Telescope-European Coordinating Facility. This new calibration process has

substantially improved the data quality and homogeneity of the FOS data. The reprocessed data have been incorporated into the *HST* Archive and are available through MAST. FOS observations have recently been cross-matched with their Hubble Source Catalog counterparts (see http://archive.stsci.edu/hst/hsc/)

C.3 Goddard High Resolution Spectrograph (GHRS)

The GHRS had two 500-element Digicon detectors that provided sensitivity from 1100 Å to 1900 Å (Side 1, solar blind) and 1150 Å to 3200 Å (Side 2); these detectors offered photon noise-limited data if an observing strategy was undertaken to map out photocathode response irregularities with the FP-SPLIT option. Signal-to-noise ratios of 100 or more were routinely achieved, and upwards of 1000 on occasion.

The GHRS modes included a first-order grating covering 1100 Å to1900 Å at R ~2500 (285 Å bandpass), four first-order holographic gratings with very low scattered light covering 1150 Å – 3200 Å at R ~25,000 (27 Å – 45 Å bandpass), and cross-dispersed echelles at R ~80,000 over 1150 Å – 3200 Å (6 Å – 15 Å bandpass).

The GHRS had two apertures: the 2.0" Large Science Aperture (LSA), and 0.25" Small Science Aperture (SSA); post-COSTAR the aperture projections were reduced to 1.74" and 0.22", respectively. The SSA projected to one resolution element; thus, even pre-COSTAR data taken with this aperture had the designed spectral resolution, albeit at reduced throughput.

Some data were acquired at time resolutions as short as 50 milliseconds in a Rapid Readout mode. Most observations were acquired in accumulation mode, which provided for oversampling, compensation for sensitivity variations along the Digicon array, and simultaneous monitoring of detector backgrounds. Routine observations of the onboard Pt-Ne emission line lamp provided data with well-calibrated wavelengths.

The GHRS received about 20% to 25% of the total *HST* observing time over Cycles 1 through 6, resulting in a large and diverse range of high quality science data. Due to the high signal-to-noise ratio and large dynamic range capabilities in the far-ultraviolet, much of these data are unique.

A major reprocessing of the entire GHRS archive (science and non-science data) has been completed by ST-ECF, CADC, and STScI. This effort substantially improves the data quality and homogeneity. For more information about the reprocessed data, see ISR GHRS-92. The reprocessed data have been incorporated into the *HST* Archive and are available through MAST. GHRS observations have recently been cross-matched with their Hubble Source Catalog counterparts (see http://archive.stsci.edu/hst/hsc/)

C.4 High Speed Photometer (HSP)

The HSP was designed to take advantage of the lack of atmospheric scintillation for a telescope in orbit, as well as to provide good ultraviolet performance. Integrations as short as 10 μs were possible over a broad wavelength range (1200 Å to 8000 Å). Observations were carried out through aperture diameters of 1.0" with the visual and ultraviolet detectors. Polarimetry was also possible with the polarimetry detector, using a 0.65" aperture.

HSP had a large variety of fixed aperture/filter combinations distributed in the focal plane; selection was accomplished by moving the telescope so as to place the target in the desired aperture behind the desired filter.

The HSP detectors consisted of four image dissector tubes and one photomultiplier tube. A variety of ultraviolet and visual filters and polarizers was available. This instrument was used for only a relatively small fraction (5%) of *HST* observing from Cycles 1 to 3 since the HSP science program was among the more severely compromised by spherical aberration. Only limited instrument expertise is available at STScI in support of HSP Archival Research. The extremely high speed with which some HSP data were acquired remains unmatched by all other *HST* instruments. GHRS observations have recently been cross-matched with their Hubble Source Catalog counterparts (see http://archive.stsci.edu/hst/hsc/).

C.5 Wide Field and Planetary Camera 1 (WF/PC)

The WF/PC had two configurations; in both channels, the field of view was covered by a mosaic of four charge-coupled devices (CCDs). Each CCD had 800 × 800 pixels and was sensitive from 1150 Å to 11,000 Å. However, internal contaminants on the camera optics limited normal operation to the range from 2840 Å to 11,000 Å.

In the Wide Field Camera (low-resolution) configuration, the field of view was 2.6' x 2.6', with a pixel size of 0.10". In the Planetary Camera (high-resolution) configuration, the field of view was 1.1' x 1.1' and the pixel size was 0.043". A variety of filters were available. The WF/PC received about 40% of the observing time on *HST* from Cycles 1 to 3, resulting in a large and diverse range of science data. All WF/PC data were severely affected by the spherical aberration. Unique and valuable data exist in the archive, but in terms of photometric accuracy, and especially image quality, imaging data taken after the first servicing mission are superior.

C.6 Wide Field and Planetary Camera 2 (WFPC2)

The WFPC2 was retired during SM4, but data from the instrument will continue to be available for archival research. It had three “wide field” CCDs and one high resolution (or “planetary”) CCD. Each CCD covered 800 x 800 pixels and was sensitive from 1150 Å to 11,000 Å. All four CCDs were exposed simultaneously, with the target of interest being placed in one of the camera apertures.

The three Wide Field Camera (WFC) CCDs were arranged in an “L”-shaped field of view whose long side projects to 2.5', with a projected pixel size of 0.10". The Planetary Camera (PC) CCD had a field of view of 35" x 35", and a projected pixel size of 0.0455". The WFC configuration provided the larger field of view, but undersampled the cores of stellar images; the PC configuration sampled the images better, but had the smaller field of view.

A total of 48 different filters could be inserted into the optical path. Polarimetry could be performed by placing a polarizer quad filter into the beam and exposing through the different quads and/or different filter wheel rotations. There were a total of 18 narrow-band and medium-band filters, as well as two narrow-band quad filters that each yielded four different central wavelengths. There were also four linear ramp filters that effectively allowed imaging of a ~10" region in an arbitrary 1.3% bandpass at any wavelength between 3700 Å and 9760 Å, by means of a variety of filter wheel orientations and target placements within the FOV.

Beginning in 2003, a serious electronic anomaly appeared in the WF4 CCD detector of WFPC2, resulting in sporadic corruption of images (which could be photometrically corrected). The frequency and severity of the problem increased slowly, and by late 2005, a significant fraction of images taken in WF4 were blank and unusable. Early in 2006, a workaround was found, which allowed good data to be taken even though the WF4 electronics continued to slowly fail. WF4 continued to produce good data for several more years. The other three CCDs appeared unaffected, and in fact, small targets were usually placed on the PC1 or WF3 CCDs, so the WF4 anomaly had much less impact than it otherwise could have.

C.7 The Advanced Camera for Surveys High Resolution Channel (ACS/HRC)

The ACS High Resolution Channel (HRC) provided high resolution, near-UV to near-IR imaging in Cycle 11 through 14. HRC observations occupied approximately 8% of all *HST* science orbits during this time. Its detector was a 1K by 1K, thinned and backside-illuminated, SITe CCD with a near-ultraviolet-optimized coating and 21 x 21 μm pixels, that provided ~0.028 x 0.025 arcsec/pixel spatial resolution. This

format yielded a nominal 29 x 26 arcsec field of view. The spectral response of the HRC ranged from ~1700 Å to ~11,000 Å, and it had a peak efficiency of 29% at ~6500 Å (including OTA throughput).

The HRC PSF was critically sampled at 6300 Å and was undersampled by a factor 3 at 2000 Å. Well-dithered observations with the HRC led to a reconstructed PSF FWHM of 0.03" at ~400 nm, which increased towards longer wavelengths.

The HRC utilized the same narrow-band and broad-band filters available with the ACS Wide Field Camera (WFC).

The HRC also offered several optics specifically designed for HRC's field of view and UV sensitivity, but also permitted vignetted WFC imaging. These HRC-specific optics included UV and visible polarizers, a prism (PR200L), three medium-broad UV filters (F330W, F250W, and F220W), and two narrow-band filters (F344N and F892N). HRC could also use the FR459M and FR914M broad ramp filters, as well as the FR505N [OIII], FR388N [OII], and FR656N (H Alpha) narrow ramp filters.

The coronagraphic mode of ACS HRC allowed high contrast imaging of faint circumstellar or circumnuclear sources, such as circumstellar debris disks and planetary companions, by preventing saturation of the detector and suppressing the diffraction pattern of the bright central source. The coronagraph featured a Lyot stop and two occulting disks that could be deployed into the field of view on demand. Finally, the HRC allowed low-dispersion (R ~100) slitless spectroscopy with the G800L grism (~23 Å/pixel in first order from 5500 Å to 10,500 Å) and the PR200L prism (~21 Å/pixel from ~3500 Å to the UV cut-off).

C.8 Near Infrared Camera and Multi-Object Spectrometer (NICMOS)

This camera provided near-infrared imaging through three independent channels. NICMOS was installed in February 1997 and had operated with a cryogenic cooling system since March 2002. NICMOS continued to operate until September 2008, when the NICMOS Cooling System (NCS) failed to cool down the instrument, following a warm-up due to a planned safemode. The instrument was not successfully restarted after Servicing Mission 4. The NCS, which was required to maintain NICMOS at its nominal operating temperature for science observations, is currently disabled.

Although the NCS was not restarted, NICMOS proposals were solicited for Cycles 18 and 19. Based upon assessments of those proposals and the efforts required to recommission NCS and NICMOS, no proposals were selected and the NCS has remained off. Therefore, NICMOS proposals are no longer being solicited.

The three NICMOS channels (NIC1, NIC2, and NIC3) provided adjacent but not spatially contiguous fields of view of different image scales; they each covered the same wavelength range from 800 nm to 2500 nm. The foci of NIC1 and NIC2 were close enough that they could be used simultaneously, whereas NIC3 had to be used by itself. NICMOS was superseded by the WFC3/IR for most infrared imaging, except for a few specialty or unique modes.

The NICMOS Camera 3 (NIC3), had the lowest spatial resolution of the three channels with a 51.2" x 51.2" field of view. The detector was a 256 x 256 HgCdTe array with 40 x 40 μm pixels. The plate scale was 0.2 arcsec/pixel. The camera did not provide diffraction-limited imaging and was operated slightly out of focus. The camera had 19 filters and one blank on a single filter wheel. Well-dithered observations with the NIC3 led to a reconstructed PSF FWHM of approximately 0.24 arcsec at 1.6 μm, increasing slightly with wavelength.

The intermediate field channel (NIC2) had a 19.2" x 19.2" field of view. The detector was a 256 x 256 HgCdTe array with 40 x 40 μm pixels. The plate scale was 0.075 arcsec/pixel. The camera provided diffraction-limited imaging at 1.75 μm and longer. The camera had 19 filters and one blank on a single filter wheel. Well-dithered observations with the NIC2 led to a reconstructed PSF FWHM of approximately 0.19 arcsec at 1.6 μm, increasing slightly with wavelength.

The narrow field channel (NIC1) had the highest spatial resolution of the three with an 11" x 11" field of view. The detector was a 256 x 256 HgCdTe array with 40 x 40 μm pixels. The plate scale was 0.043 arcsec/pixel. The camera provided diffraction-limited imaging longward of 1 μm. The camera had 19 filters and one blank on a single filter wheel. Well-dithered observations with the NIC1 led to a reconstructed PSF FWHM approximately 0.14 arcsec at 1.6 μm, increasing slightly with wavelength.

In the near-infrared, NICMOS was unique in providing imaging polarimetry and coronagraphy. NICMOS also provided HST's only capabilities longward of 1700 nm including access to the Pa line and K band. Furthermore the ability to defocus the NICMOS grisms had enabled spectroscopy of bright targets. NICMOS had grisms for slitless spectroscopy.

APPENDIX D:

Internet Links

Web Links

ACS Dither Website

http://www.stsci.edu/hst/acs/proposing/dither

ACS Instrument

http://www.stsci.edu/hst/acs/

ACS Instrument Handbook

http://www.stsci.edu/hst/acs/documents/handbooks/current/cover.html

Aladin Sky Atlas

http://aladin.u-strasbg.fr/

Anderson J. & Bedin, L. R., 2010, PASP, 122, 1035

http://adsabs.harvard.edu/abs/2010PASP.122.1035A

APT Training Materials Webpage

http://www.stsci.edu/hst/proposing/apt/using_apt

APT Webpage

http://www.stsci.edu/hst/proposing/apt

Astronomer's Proposal Tool (APT)

http://www.stsci.edu/hst/proposing/apt

Budavári, T. & Lubow, H.S., 2012ApJ...761..188B

http://adsabs.harvard.edu/abs/2012ApJ...761..188B

Canadian Astronomy Data Centre (CADC)

http://cadcwww.hia.nrc.ca/

COS Instrument Website

http://www.stsci.edu/hst/cos/

COS Instrument Handbook

http://www.stsci.edu/hst/cos/documents/handbooks/current/cos_cover.html

Cycle 25 Announcement Webpage

http://www.stsci.edu/hst/proposing/docs/cycle25announce

Cycle 25 Call for Proposals

http://www.stsci.edu/hst/proposing/documents/cp/cp_cover.html

Digitized Sky Survey (DSS)

http://archive.stsci.edu/dss/

DrizzlePac Handbook

http://documents.stsci.edu/hst/HST_overview/documents/DrizzlePac/DrizzlePac.cover.html

DrizzlePac Website

http://drizzlepac.stsci.edu

ESA Hubble Science Archive

http://archives.esac.esa.int/hst/

Exposure Time Calculators Website

http://etc.stsci.edu/

Fine Guidance Sensor Instrument

http://www.stsci.edu/hst/fgs/

Fine Guidance Sensor Instrument Handbook

http://www.stsci.edu/hst/fgs/documents/instrumenthandbook

High Level Science Products

http://archive.stsci.edu/hlsp/index.html

Hubble Legacy Archive (HLA)

http:///hla.stsci.edu

Hubble Source Catalog (HSC)

https://archive.stsci.edu/hst/hsc/

HST Data Handbook

http://www.stsci.edu/hst/HST_overview/documents/datahandbook/

HST Documents Webpage

http://www.stsci.edu/hst/HST_overview/documents

HST Dither Handbook

http://www.stsci.edu/hst/HST_overview/documents/dither_handbook

HST Instrument Handbooks

http://www.stsci.edu/hst/HST_overview/documents

HST Online

http://archive.stsci.edu/hstonline/search.php

HST Science Instruments

http://www.stsci.edu/hst/HST_overview/instruments

Image Reduction and Analysis Facility (IRAF)

http://iraf.noao.edu/

MAST Discovery Portal (DP)

http://mast.stsci.edu/portal

Mikulski Archive for Space Telescopes (MAST)

http://archive.stsci.edu/

MultiDrizzle

http://stsdas.stsci.edu/multidrizzle/

NASA/IPAC Extragalactic Database (NED)

http://nedwww.ipac.caltech.edu/

NICMOS Instrument

http://www.stsci.edu/hst/nicmos/

NICMOS Instrument Handbook

http://www.stsci.edu/hst/nicmos/documents/handbooks/current_NEW/cover.html

Parallel Observations

http://www.stsci.edu/hst/HST_overview/documents/uir/UIR_Parallels.pdf

Phase I Proposal Roadmap

http://apst.stsci.edu/apt/external/help/roadmap1.html

Phase II Program Preparation

http://www.stsci.edu/hst/programs

PyRAF

http://www.stsci.edu/resources/software_hardware/pyraf

Set of Identifications, Measurements and Bibliography for Astronomical Data (SIMBAD)

http://simbad.u-strasbg.fr/Simbad

Space Telescope - European Coordinating Facility

http://www.stecf.org/

Space Telescope Science Data Analysis Software (STSDAS)

http://www.stsci.edu/resources/software_hardware/stsdas

Space Telescope Science Institute

http://www.stsci.edu/

STIS Instrument

http://www.stsci.edu/hst/stis/

STIS Instrument Handbook

http://www.stsci.edu/hst/stis/documents/handbooks/currentIHB/stis_ihbTOC.html

Tiny Tim

http://www.stsci.edu/software/tinytim/

Visit Size Recommendations

http://www.stsci.edu/hst/programs/recommendations

WFC3 Instrument

http://www.stsci.edu/hst/wfc3/

WFC3 Instrument Handbook

http://www.stsci.edu/hst/wfc3/documents/handbooks/currentIHB/wfc3_cover.html

WFC3 UVIS CTE Webpage

http://www.stsci.edu/hst/wfc3/ins_performance/CTE/

WFPC2 Instrument

http://www.stsci.edu/hst/wfpc2/

WFPC2 Instrument Handbook

http://documents.stsci.edu/hst/wfpc2/documents/handbooks/cycle17/wfpc2_cover.html

Instrument Science Reports

ACS ISR 06-04

http://www.stsci.edu/hst/acs/documents/isrs/isr0604.pdf

ISR FOC-99

http://www.stsci.edu/ftp/instrument_news/FOC/Foc_isr/foc_isr099

ISR GHRS-92

http://www.stsci.edu/hst/ghrs/documents/isrs/ghrs_isr092.pdf

STIS ISR 2011-02

http://www.stsci.edu/hst/stis/documents/isrs/201102.pdf

WFC3 ISR 2009-30

http://www.stsci.edu/hst/wfc3/documents/ISRs/WFC3-2009-30.pdf

WFC3 ISR 2009-31

http://www.stsci.edu/hst/wfc3/documents/ISRs/WFC3-2009-31.pdf

WFC3 ISR 2009-40

http://www.stsci.edu/hst/wfc3/documents/ISRs/WFC3-2009-40.pdf

WFC3 ISR 2009-47

http://www.stsci.edu/hst/wfc3/documents/ISRs/WFC3-2009-47.pdf

WFC3 ISR 2010-09

http://www.stsci.edu/hst/wfc3/documents/ISRs/WFC3-2010-09.pdf

WFC3 ISR 2010-14

http://www.stsci.edu/hst/wfc3/documents/ISRs/WFC3-2010-14.pdf

WFC3 ISR 2011-08

http://www.stsci.edu/hst/wfc3/documents/ISRs/WFC3-2011-11.pdf

WFC3 ISR 2012-08

http://www.stsci.edu/hst/wfc3/documents/ISRs/WFC3-2012-08.pdf

APPENDIX E:

Glossary of Acronyms and Abbreviations

ACQ	Acquisition
ACS	Advanced Camera for Surveys
ACS/HRC	ACS High Resolution Camera
ACS/SBC	ACS Solar Blind Channel
ACS/WFC	ACS Wide Field Camera
APT	Astronomer's Proposal Tool
BOP	Bright Object Protection
CADC	Canadian Astronomy Data Centre
CCD	Charge-Coupled Device
COS	Cosmic Origins Spectrograph
COS/FUV	COS Far-Ultraviolet Channel
COS/NUV	COS Near-ultraviolet Channel
COSTAR	Corrective Optics Space Telescope Axial Replacement
CTE	Charge Transfer Efficiency
CVZ	Continuous Viewing Zone
DADS	Data Archive and Distribution System
DD	Director's Discretionary
DQE	Detector Quantum Efficiency
DSS	Digitized Sky Survey
ESA	European Space Agency
ETC	Exposure Time Calculator

FGS	Fine Guidance Sensor(s)
FITS	Flexible Image Transport System
FOC	Faint Object Camera
FOS	Faint Object Spectrograph
FOV	Field of View
FUV	Far Ultraviolet
GHRS	Goddard High Resolution Spectrograph
GO	General Observer
GSC	Guide Star Catalog
GSFC	Goddard Space Flight Center
GTO	Guaranteed Time Observer
HLA	Hubble Legacy Archive
HLSP	High Level Science Products
HSC	Hubble Source Catalog
HSP	High Speed Photometer
HST	Hubble Space Telescope
HTML	Hyper Text Markup Language
IFOV	Instantaneous field of view
IRAF	Image Reduction and Analysis Facility
ISR	Instrument Science Report
LRF	Linear Ramp Filter
MAMA	Multi-Anode Microchannel Array
mas	milli arcsecond
MAST	Multi-mission Archive at STScI
NASA	National Aeronautics and Space Administration
NED	NASA/IPAC Extragalactic Database
NCS	NICMOS Cooling System
NICMOS	Near Infrared Camera and Multi-Object Spectrometer
NOAO	National Optical Astronomy Observatories
NUV	Near Ultraviolet
OMS	Observatory Monitoring System
OTA	Optical Telescope Assembly
OTFR	On-The-Fly Reprocessing

PAM	Pupil Alignment Mechanism
PC	Planetary Camera
PCS	Pointing Control System
PDF	Portable Document Format
PI	Principal Investigator
POS	Position Mode
PSF	Point Spread Function
SAA	South Atlantic Anomaly
SAM	Small Angle Maneuver
SI	Scientific Instrument
SIMBAD	Set of Identifications, Measurements and Bibliography for Astronomical Data
SM	Servicing Mission
SSM	Support Systems Module
SSR	Solid State Recorder
ST-ECF	Space Telescope - European Coordinating Facility
STIS	Space Telescope Imaging Spectrograph
STIS/CCD	STIS CCD Detector
STIS/FUV-MAMA	STIS Far Ultraviolet Channel
STIS/NUV-MAMA	STIS Near Ultraviolet Channel
STOCC	Space Telescope Operations Control Center
STScI	Space Telescope Science Institute
STSDAS	Space Telescope Science Data Analysis Software
TDRSS	Tracking and Data Relay Satellite System
TRANS	Transfer Mode
UIR	User Information Report
UV	Ultraviolet
VIK	Voltage/Temperature Improvement Kit
WFC	Wide Field Camera (on WFPC2) or Wide Field Channel (on ACS)
WFC3	Wide Field Camera 3
WFC3/IR	WFC3 High-Throughput Infrared Channel
WFC3/UVIS	WFC3 Ultraviolet-Visible Channel
WF/PC	Wide Field and Planetary Camera 1
WFPC2	Wide Field and Planetary Camera 2